Charles University
Faculty of Mathematics and Physics

Doctoral Thesis

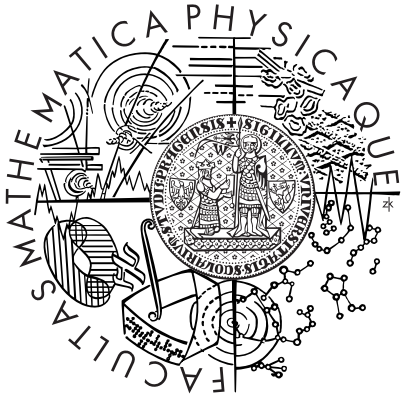

Role of Magnetosheath Parameters on Magnetopause Processes

Oksana Tkachenko

Department of Surface and Plasma Science

Supervisor: Prof. RNDr. Jana Šafránková, DrSc.

Study Branch: f-2

Prague 2011

Acknowledgments

It is a pleasure to thank those who made this thesis possible. I am heartily thankful to my principal and secondary supervisors, Prof. Jana Šafránková and Prof. Zdeněk Němeček, whose guidance, encouragement and support from the initial to the final level enabled me to complete this work. With their enthusiasm, inspiration and great efforts to explain things clearly and simply, they helped to challenge fascinating world of Space Physics.

I want to thank Dr. Lubomír Přech for valuable advises in programming, help with data acquisition and data handling and also for his assistance with all types of technical problems – at all times. I also warmly thank Jiří Pavlů for his help with the organizational matters and Karel Jelínek for help in programming especially at the beginning of my study. I would like to acknowledge Charles University teacher team who improve my knowledge in the plasma physics, for numerous interesting discussions and lectures on related topics over the course of my Ph.D.

I am forever indebted to my parents for their endless love and devotion. I dedicate this thesis to my Dad who always believed in me and will be example to follow for all my life. I would like to express special gratitude to my beloved, Vratislav, for his love and support though this long path. His valuable advises help me in deadlock situations and your criticism encourage me to improve myself.

Last but not the least, I wish to thank all my friends for providing a pleasant and fun environment during last four years.

I, Oksana Tkachenko, confirm that the work presented in this thesis is my own. If information has been derived from other sources, I confirm that it has been indicated in the thesis.

March 20, 2011 in Prague Oksana Tkachenko

Abstract

Title: *Role of magnetosheath parameters on magnetopause processes*

Author: *Oksana Tkachenko*

Department: *Department of Surface and Plasma Science*

Supervisor: *Prof. RNDr. Jana Šafránková, DrSc.*

e-mail address: *Jana.Safrankova@mff.cuni.cz*

Abstract: *The thesis addresses of two regions significant for the solar wind-magnetosphere coupling: the cusp in high geomagnetic latitudes and the low-latitude (LLBL) subsolar magnetopause. A penetration of plasma of a solar origin into the magnetosphere could be realized directly through magnetospheric cusps. The region adjacent to the magnetopause in the cusp vicinity is highly turbulent, occupied by the heated magnetosheath–like plasma with a low drift velocity for which occurrence of vortices is a very common feature. In the first part of the thesis, we present a detailed analysis of a vortex-like structure created by a turbulent plasma flow around the magnetopause indentation above the cusp and using the data from Interball-1 and Magion-4; we find necessary conditions and a possible mechanisms to creation of such structures. The second part concerns the low–latitude boundary layer formation, its spatial structure and temporal changes based on THEMIS multipoint observations. In spite of its crucial role in transfer of mass, momentum, and energy from the solar wind into the magnetosphere, LLBL parameters and their relations to upstream conditions are still under debate. We demonstrate that sudden changes in upstream plasma and magnetic field parameters could lead to reformation of the spatial LLBL profile from smooth to apparently non-monotonous. Disturbances at the magnetopause surface suggested to be the main reason of the distortion of the spatial structure of this layer. In details, we study LLBL passages in order to determine sources of transient events. A monitor of magnetosheath parameters is principal for an interpretation of magnetopause transients. It was found that the changes of the B_Z sign could be a cause of the magnetopause deformation and could reform the LLBL.*

Keywords: *solar wind, magnetosheath, magnetopause, interplanetary magnetic field, cusp, low-latitude boundary layer, reconnection*

Abstrakt

Název práce: *Vliv parametrů přechodové oblasti na magnetopauzové procesy*

Autor: *Oksana Tkachenko*

Katedra: *Katedra fyziky povrchů a plazmatu*

Vedoucí disertační práce: *Prof. RNDr. Jana Šafránková, DrSc.*

e-mail address: *Jana.Safrankova@mff.cuni.cz*

Abstrakt: *Předkládaná dizertační práce je zaměřena na dvě oblasti, jež jsou důležité pro interakci slunečního větru s zemskou magnetosférou: kasp ve vysokých geomagnetických šířkách a subsolární magnetopauza v nízkých šířkách. Průnik slunečního plazmatu do zemské magnetosféry může probíhat podél kaspů. Oblast přilehlá k magnetopauze v blízkosti kaspu je velmi turbulentní, vyplněná horkým plazmatem z přechodové oblasti s nízkou driftovou rychlostí. V první části dizertační práce se proto věnujeme detailnímu rozboru vírové struktury ve vhloubení magnetopauzy nad kaspem za použití dat družic Interball–1 a Magion–4. Popsali jsme nezbytné podmínky a možný mechanismus vzniku této struktury. Druhá část práce se týká formování a prostorové struktuře hraniční vrstvy nízkých šířek (Low-latitude Boundary Layer, dále LLBL) a jejím časovým změnám. Ačkoliv LLBL hraje klíčovou roli v přenosu hmoty, hybnosti a energie ze slunečního větru do magnetosféry, její změny a vlastnosti nejsou doposud přesně popsány. Na datech z pěti družic projektu THEMIS ukazujeme, že náhlé změny parametrů slunečního větru a meziplanetárního magnetického pole mohou vést ke změnám prostorového profilu LLBL z hladkého na zdánlivě nemonotonní. Příčinou tohoto jevu jsou poruchy na povrchu magnetopauzy. Podrobně jsme prozkoumali průlety družic vrstvou LLBL, abychom určili zdroje těchto poruchových událostí. Dokázali jsme, že principiální jsou změny, ke kterým dochází v přechodové oblasti. Zjistili jsme že změny směru magnetického pole ze severního na jižní (a naopak) jsou příčinou deformace povrchu magnetopauzy a mohou změnit tvar LLBL.*

Klíčová slova: *sluneční vítr, přechodová oblast, magnetopauza, meziplanetární magnetické pole, kasp, hraniční vrstva nízkých šířek, rekonekse*

Contents

Chapter 1

Introduction

Space and space phenomena fascinate human mind since the very beginning of our existence on the Earth. We have passed a long way in exploration of the Universe and our place in it, from the many centuries of ground observations of the celestial bodies to multi-spacecraft missions to the edge of the Solar System. An influence of the Sun and its activity on the Earth is ultimately proved. Nowadays, space technologies play a significant role in our scientific research shifting the outer limits of our knowledge. Due to the development of spacecraft technology, *in situ* observations of the plasma and magnetic field in the magnetosphere and interplanetary medium become possible.

During last sixty years, there has been numerous missions with various objectives that collected data from different regions within the Solar System. Multi-spacecraft measurements near the Earth give us the opportunity to enhance the knowledge of the interaction between the solar wind and magnetosphere, allow us to distinguish with a significant resolution spatial and temporal structures of particular regions. Sun ejects continuous plasma flow (the solar wind) with the frozen-in magnetic field as well as it is a source of the energetic particles and different types of electromagnetic waves. The Earth's magnetosphere is formed under the interaction of the solar wind with the terrestrial magnetic field. Thin current sheet, the magnetopause, separates two media and prevents the penetration of the solar wind into the magnetosphere. The solar wind with the interplanetary magnetic field modifies the shape of the magnetosphere by pushing it on the dayside and creating a long magnetotail on the nightside. There are two cusps, funnel-shaped regions with near zero magnetic field magnitude in the vicinity of the magnetic poles, where the solar plasma has direct access to the upper ionosphere. The cusps are believed to be key regions for the transfer of mass, momentum, and energy from the solar wind into the magnetosphere. The penetration of the plasma of a solar origin into the magnetosphere could be realized as well through magnetic reconnection at the dayside magnetopause. A position of the reconnection site moves in accord with an actual interplanetary magnetic field direction. The processes leading to the plasma crossing the Earth's magnetopause and forming a low-latitude boundary layer (LLBL) are not fully known but their understanding is important for determination of physical

processes in the magnetosphere.

For this reason, the thesis addresses these two key regions: the cusp in high geomagnetic latitudes and the low-latitude subsolar magnetopause.

This thesis was prepared under a support of the Research Plan MSM 0021620860 that is financed by the Ministry of the Education of the Czech Republic.

Chapter 2

Solar-Terrestrial Relationship

2.1 Solar Wind-Magnetosphere Coupling

The solar wind is a flow of ionized solar plasma ejected from the Sun with the residue of the solar magnetic field that fills up interplanetary space. The first *in situ* observations of the solar wind were made in the 1960s (Lunik 2 and 3). However, the existence of a continuous particle flow from the Sun had been suggested in 1908 by *Birkeland* in order to explain the connection between the sunspots activity and particles precipitation on the Earth, known as northern light or aurora borealis. Another observational evidence for this assumption was deduced from the properties of cometary tails by *Biermann and Schlüter* (1951). They were noted that comets have two tails; dust tail directed along its trajectory, and plasma tail deviated several degrees from the solar radial direction (away from the Sun). The second one is shaped by the solar particles not by the solar light pressure. *Chapman and Zirin* (1957) calculations of the solar corona parameters predicted that the corona should extend further into space than the orbit of the outermost planet. The solutions of the fluid equations describing the solar atmosphere demonstrated by *Parker* (1958) confirm the necessity of the existence of a continuous solar wind that accelerates with a radial distance outward the Sun becoming supersonic. The solar wind disturbances are mainly driven by the solar activity or, in another words, by changes in the solar magnetic field. The solar wind research is important in order to understand how this expanding plasma transmits the influence of the solar activity to planets, comets and dust particles.

The generation mechanisms of the solar wind are complicated and in some simplified sense, it is a result of a huge difference in gas pressure between the solar corona and interstellar space. Emitted plasma particles are accelerated in the hot (1.6×10^6 K) and dense (5×10^{17} cm^{-3}) solar corona and then sweep outward. An origin of such high temperature of the corona remains still under debate. The solar wind consists mainly of protons and electrons, with a small amount of heavier elements (5% of helium ions and heavier species). Extensive measurements of the solar wind were made by the spacecraft in the vicinity of the Earth. The density of the ionized gas at 1 AU is typically about 5 cm^{-3}.

The proton temperature is of order 10^5 K while the electron temperature is a little bit hotter. The value of the embedded magnetic field is near 5 nT. The speed range of the solar wind is from a couple of hundreds km/s to 1400 km/s. The flow is directed radially from the Sun with a small deviation ($< 5°$) caused by an orbital motion of the Earth. There are two distinct types of the solar plasma flow (Figure 2.1a): the slow solar wind has velocities $\sim$ 300 – 450 km/s and fast has velocities of about 500 – 900 km/s (*Phillips et al.*, 1995). The fast solar wind is stable over a long period with small variations. The ion density is about 3 cm^{-3} at 1 AU. It originates from the coronal holes characterized by open field lines. The temperature of a fast stream is about 8×10^5 K and it matches the composition of the photosphere of the Sun. By contrast, the slow solar wind has lower speed, lower temperature that is about $\sim 1.5 \times 10^5$ K, and density is about twice as large as that in the fast solar wind. The slow solar wind originates from regions close to the current sheet at the heliomagnetic equator during solar minimum, and above the active regions in the streamer belt during solar maximum. The slow wind has a complex structure, it is highly variable and often contains large-scale structures such as magnetic clouds or interplanetary shocks.

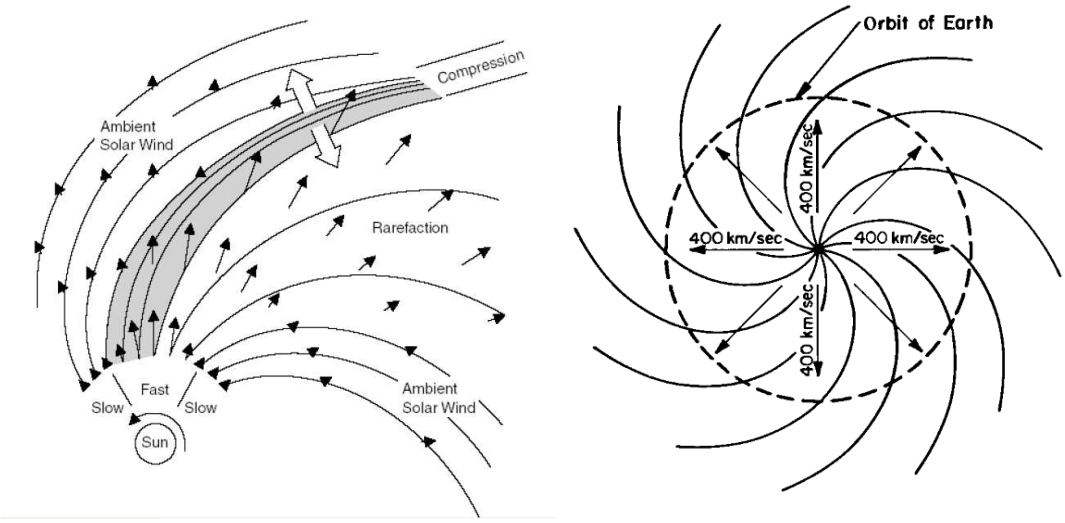

(a) (b)

Figure 2.1: (a) Geometry of the interaction between the fast and slow solar wind. The plasma is compressed where streamlines converge (adapted from *Pizzo*, 1985). (b) The Parker spiral assuming a constant solar wind radial speed of 400 km/s, and a radial magnetic field at the solar surface (from *Kivelson and Russell*, 1995). The solar wind flows radially outward from the Sun as the Sun rotates. This causes a spiral orientation of the IMF.

As the solar wind plasma has a high electrical conductivity, the magnetic field lines of solar origin are carried along the flow. This frozen-in magnetic field is called the interplanetary magnetic field (IMF). As it was aforementioned, the

typical magnitude of the IMF at 1 AU is about 5–10 nT. Although the solar wind flows radially from the Sun with domination of the dynamic pressure in the wind over the magnetic pressure, the rotation of the Sun causes the magnetic field lines to form the Archimedean or "Parker" spiral (Figure 2.1b) that was firstly suggested by *Parker* (1958).

Rotation period of the Sun is about 26 days, and thus the field lines are inclined by 45° with respect to the flow at 1 AU. Depending on the Sun hemisphere and phase of the solar cycle, the radial component of the IMF is directed inward or outward. The measurements made by IMP–1 in 1963 reveal a sector pattern of the magnetic field polarity. During each solar rotation near the solar minimum, either two or four sectors can be observed. In this sectors, the magnetic field polarity is uniform over a large angular region and then abruptly changes polarity. Such reverse in the radial direction of the IMF is defined by the variations of the neutral line inclination. During maximum of the solar activity, the sectoral structure is more complicated and is influenced by a large number of transient disturbances. The IMF variations control many aspects of the solar wind/magnetosphere interaction, especially its z component (perpendicular to the ecliptic). Models of the global structure of the solar wind have become sufficiently detailed and sophisticated. A detailed discussion of the solar wind properties can be found in *Hundhausen* (1995), *Velli* (2001).

2.2 Magnetosphere and Its Boundaries

2.2.1 Bow Shock and Magnetosheath

The Earth's magnetic field that forms the magnetosphere presents an obstacle for the solar wind (*Chapman and Ferraro*, 1930). The IMF cannot penetrate into the terrestrial magnetic field cavity as well as the solar wind particles. The boundary separating the magnetosphere from the solar wind is called the magnetopause.

Since the solar wind plasma is supersonic, a shock wave (the bow shock) is generated upstream of the Earth. The solar wind speed is slowed down to subsonic at the bow shock in order to pass around the Earth, the shock should move away from the obstacle to the point where the compressed solar wind can move between the shock and the magnetopause. When the shock weakens, the compression ratio across the shock decreases to unity (no compression) and the shock moves to infinity. The position, shape and motion of the bow shock have been extensively studied resulting in many bow shock models (*e.g.*, *Formisano*, 1979, *Němeček and Safrankova*, 1991, *Farris and Russell*, 1994, *Jeřáb et al.*, 2005). These models usually combine the gasdynamic or magnetohydrodynamic theory with spacecraft observations.

Behind the bow shock, the piled up plasma compresses, therefore the plasma density increases. The plasma temperature also increases across the shock because a larger part of the bulk kinetic energy of the solar wind is converted to thermal energy. This region of shocked, dense plasma of solar wind origin is called the magnetosheath. Typical plasma densities are 10-30 cm^{-3}, velocities

200 km/s and particle energies are of order 10-100 eV for electrons and ∼1 keV for ions. Since the plasma density in the magnetosheath is greater than in the solar wind, and the magnetic field is frozen into the plasma, the magnetic field magnitude is also larger compared with the IMF (magnetic field strength is about 30–40 nT).

The magnetosheath is a highly turbulent region with a plenty of various waves, boundaries and shocks (discontinuities). The magnetosheath turbulence is considered as a mixture of the linear wave modes, Alfven-ion-cyclotron and mirror waves, generated by unstable ion distributions.

Fluctuations in the plasma and magnetic field parameters are very typical for magnetosheath, and may be caused by the solar wind features like shocks and tangential discontinuities or different types of waves. Variations can also be due to the radial gradient of the parameters combined with radial motion of the bow shock–magnetosheath–magnetopause system, which can be driven by changes in the IMF orientation (*Sibeck and Gosling*, 1996).

Since upstream variations in the solar wind plasma can be significantly modified upon traversing the magnetosheath, the magnetosheath region itself is difficult to simulate. *Spreiter et al.* (1966) used gas-dynamic model to describe the plasma flow inside the magnetosheath. Later several theoretical models have been developed to understand the evolution of the plasma and magnetic field properties in this transition region (*Zwan and Wolf*, 1976, *Southwood and Kivelson*, 1995). Recent development of new numerical methods leads to new MHD models, *e.g.*, BATS-R-US (http://csem.engin.umich.edu/docs/), that simulate the MHD properties better than the gas–dynamic model. Nowadays, the MHD models describe magnetosheath parameter changes qualitatively and quantitatively (local models).

The angle between the magnetosheath and magnetospheric magnetic fields defines the magnetic shear angle across the magnetopause. When the magnetic shear is low ($< 30°$), a magnetosheath transition layer, also called the "plasma depletion layer" is formed just outside the magnetopause (*Crooker et al.*, 1979, *Fuselier et al.*, 1991, *Wang et al.*, 2004). The magnetic field direction inside the magnetosheath is important also for the proposed merging process with the geomagnetic field.

2.2.2 Magnetopause

At the inner edge of the magnetosheath, the shocked solar wind flow encounters the magnetopause: a thin current layer shielding out the magnetospheric magnetic field from IMF. These currents are named the Chapman-Ferraro currents. The first simple model for the structure of the magnetopause current was proposed by *Ferraro* (1952) (see Figure 2.2). The thickness of this current sheet should be around the ion gyro radius (∼1000 km).

The dynamic pressure of the solar wind and the direction of IMF are the most important factors controlling position and shape of the magnetopause. The magnetopause stands off the shocked solar wind flow at locations where the sum

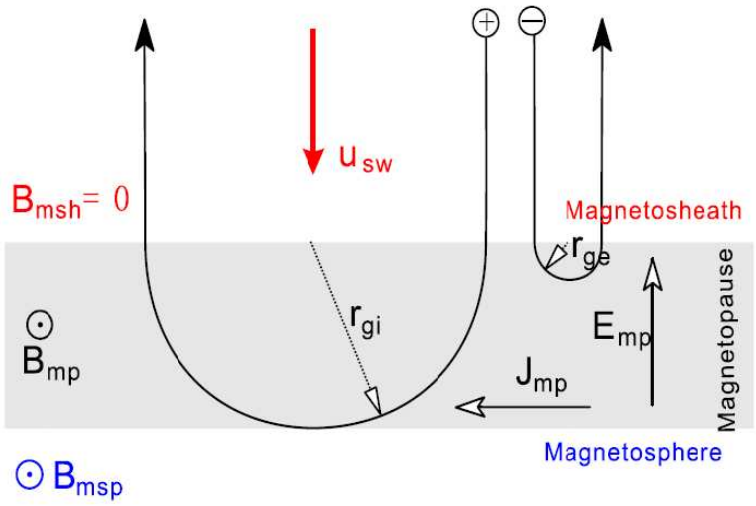

Figure 2.2: A simple magnetopause current model proposed by *Ferraro* (1952). When solar wind particles encounter the Earth's field, they are bent from their paths by the Lorentz force. Protons gyrate in a left-handed sense around a magnetic field and electrons in a right-handed sense, forming a current flowing from dawn to dusk.

of the thermal and magnetic pressures in the magnetosheath and magnetosphere are in balance. A typical value for the location of the magnetopause subsolar point (the nearest point to the Sun) is at ∼10–12 R_E (1 R_E (Earth's radius)=6371 km) from the Earth center, while on the flanks the magnetopause is located at a distance ∼15 R_E. The distant tail of the magnetosphere has a circular cross-section with a radius of ∼25–30 R_E.

Various models of the magnetopause have been proposed in the past and allow us to obtain a quantitative relation between the size and shape of the magnetopause and the solar wind parameters. According to the classical Chapman-Ferraro theory, the magnetopause position can be derived from the pressure balance between the solar wind dynamic pressure, p, and the magnetic pressure of the geomagnetic field:

$$(p)_{upstream} = \left(\frac{B^2}{2\mu_0}\right)_{downstream} \tag{2.1}$$

where B is the geomagnetic field and μ_0 is permeability of vacuum. Therefore the magnetopause standoff distance, at least at the dayside, should vary as $p^{-1/6}$. Some authors suggest that the IMF orientation also influences the shape and location of the magnetopause. The magnetopause moves inward with an increasing of the cross-section in the magnetospheric tail during periods of southward IMF. Thus, recent empirical magnetopause models are parametrized by both the solar wind dynamic pressure p and IMF B_Z (*e.g.*, *Roelof and Sibeck*, 1993, *Petrinec and Russell*, 1993, 1996, *Shue et al.*, 1997, 1998). Some of these models used inverse trigonometric functions whereby others models adopted either the general

equation of an ellipsoid with two parameters (eccentricity and standoff distance) or the general quadratic equation. *Shue et al.* (1997) used the standoff distance and the level of tail flaring. *Boardsen et al.* (2000) presented a new empirical model for the shape of the near-Earth high-latitude magnetopause where added as a parameter dipole tilt angle.

Since in this thesis the *Shue et al.* (1997) model was used for the determination of the magnetopause location, a brief description is presented. A functional form that has a sufficient flexibility to fit the magnetopause size and shape is:

$$r(\theta) = r_0 \left(\frac{2}{1 - \cos(\theta)} \right)^{\alpha}, \tag{2.2}$$

where r_0 and α are the standoff distance and the level of tail flaring, respectively. The coefficients r_0 and α are defined as:

$$\alpha = (0.58 - 0.01 B_Z)(1 + 0.01 p_{SW}), \tag{2.3}$$

$$r_0 = \frac{11.4 + m_1 B_Z}{\sqrt[6.6]{p_{SW}}}, \tag{2.4}$$

where $m_1 = 0.13$ for $B_Z > 0$ and $m_1 = 0.14$ for $B_Z < 0$.

2.2.3 Inner and Outer Magnetosphere

The magnetosphere is a highly dynamic system, containing regions with different properties. The magnetosphere may be divided into several broad regions such as the boundary layers, plasmasphere, plasma mantle, plasma sheet.

The regions of the magnetosphere and magnetospheric currents are illustrated in Figure 2.3. Moving radially outwards from the Earths surface, three overlapping particle populations can be found in this region: the ionosphere, plasmasphere and radiation belts. The ionosphere consists of the fraction of the terrestrial atmosphere which is ionized by solar UV radiation. At higher altitudes (above 80 km), the atmosphere is rare enough, thus collisions between particles and free electrons are infrequent and recombination occurs at a low enough rate to allow a permanently ionized population. Above the ionosphere, the plasmasphere lies at low and middle latitudes. The boundary between the ionosphere and plasmasphere is not clearly defined, but the plasmasphere has a lower density. The outer limit of the plasmasphere, where the density drops down sharply from 10^3 to 1 cm^{-3}, is called the plasmapause. Magnetospheric field lines are often referred to by their L-shell number, which is the radial distance (in R_E), from the center of the Earth at which they cross the equatorial plane; the plasmapause lies at about L = 4.

The magnetic field lines which contain the plasma sheet population map down to the atmosphere at high latitudes and define the auroral oval. Here, energetic plasma sheet particles collide with each other and excite the electrons of neutral atoms/molecules. When the excited electrons relax, light at distinct wavelengths (both ultraviolet and visible) is emitted. These lights are the aurora.

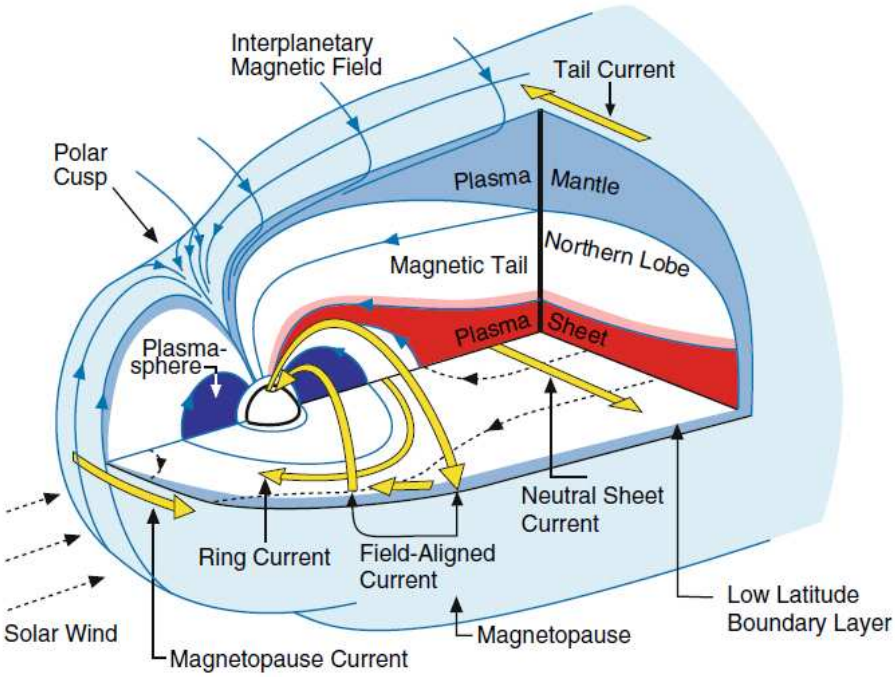

Figure 2.3: Three-dimensional cutaway view of the magnetosphere. The light blue outer surface is the magnetopause, its boundary layers are shown in darker blue. Magnetic field lines are shown in blue, electric currents in yellow. The polar region where the magnetic field lines converge is the polar cusp (from *Kivelson and Russell* (1995)).

The radiation (or van Allen) belts consist of energetic electrons and ions which are trapped on magnetic field lines between 2<L<6. The inner one located between about 1.1–3.3 R_E in the equatorial plane contains primarily protons with energies exceeding 10 MeV. A source of these protons is the decay of cosmic rays induced reflection from the atmosphere. The outer belt contains mainly electrons with energies up to 10 MeV. It has an equatorial distance of about 3–9 R_E and is produced by injection and energization events following geomagnetic storms, which make it much more dynamic than the inner belt. The radiation belts are of importance primarily because of the harmful effects of high–energy particles and radiation for man and electronics.

On the night-side of the Earth, the magnetosphere is extended into a structure called the magnetotail. The region of space containing field lines connected to higher latitude regions is called the lobe. Field lines of the lobes are smooth, and maintain roughly the same direction until they converge above the poles. They point towards Earth north of the equator and away from Earth south of it. The electron density in the lobe is particularly low ($\gg 0.01$ cm^{-3}), and the magnetic field, which extends predominantly anti-sunward in the southern hemisphere, and sunward in the northern hemisphere, has typical magnitude of about 30 nT.

At low latitudes, there is a thick region called the plasma sheet where locates the most of the magnetotail plasma; electron densities of 1 cm^{-3} and energies of several keV are observed. The plasma sheet magnetic field strength is of order 10 nT.

The outer magnetospheric boundary layer is a region close to the magnetopause in which magnetosheath plasma has strong influence. It can be divided into four main parts: the plasma mantle, LLBL, entry layer and exterior cusp or stagnation region. Since a small fraction of the oncoming shocked solar wind plasma crosses the magnetopause, it forms a magnetospheric boundary layer whose thickness increases from about 1000 km on the dayside to as much as several R_E on the magnetospheric flanks. This layer has different characteristics at low and high latitudes. Whereas the equatorial LLBL contains a mixture of magnetospheric and magnetosheath plasmas and appears to lie on a combination of open and closed magnetic field lines, the high-latitude plasma mantle contains mainly a magnetosheath plasma with depressed densities and appears to lie entirely upon open magnetic field lines (one end on Earth, the other in the solar wind).

Earth's cusps are magnetic field features in the magnetosphere associated with regions through which magnetosheath plasma has direct access to the upper atmosphere. The cusp is a region of nearly-stagnant dense (5 to 10 cm^{-3}) magnetosheath-like plasma on high-latitude magnetospheric magnetic field lines which map to the magnetopause. The cusp separates field lines near local noon which trace to the dayside magnetosphere and those which map to the nightside. The energetic ions ($\sim$ 1 keV) can be frequently observed in the magnetosheath up to several thousand kilometers from the magnetopause, and occasionally much further upstream in the solar wind, whereas escaping electrons are generally confined to the immediate vicinity of the magnetopause.

The cusp's position and size depend on many upstream as well as magnetospheric parameters, *i.e.*, the cusp location changes in response to changes in the orientation of the Earth's dipole axis, the solar wind dynamic pressure, and IMF orientation (*Newell and Meng*, 1987, 1989, *Zhou et al.*, 1999, *Němeček et al.*, 2000, *Merka et al.*, 2002). Based on a statistical study from the DMSP satellites by *Newell et al.* (1989), the cusp moves equatorward (poleward) when IMF turns southward (northward). As the IMF B_Y component becomes more negative, the cusp moves to earlier local times in the northern hemisphere. This is consistent with a motion of the reconnection site away from the noon meridian when the IMF is not pure southward (*Crooker*, 1979, *Russell et al.*, 2000). When IMF is positive, the northern cusp moves to later local times. When the solar wind dynamic pressure increases the polar cusp becomes wider in both local times and latitudes and moves equatorward as a result of its global expansion (*Newell and Meng*, 1994).

2.3 Plasma Transfer Processes at the Magnetopause

The magnetopause is an highly important region because the physical processes at this boundary control the entry of the solar plasma, momentum, and energy into the magnetosphere. Several sources of the LLBL plasma and mechanisms of plasma penetration through the magnetopause were suggested over the years. Qualitatively, the plasma transport across the magnetopause evolves magnetic field reconnection, diffusion, Kelvin-Helmholtz instabilities, impulsive penetration.

2.3.1 Magnetic Field Reconnection

Magnetic reconnection is a fundamental process in a magnetized plasma, whereby the magnetic energy is converted into kinetic energy. In the MHD approximation, magnetized plasmas of different origin come into contact, cannot mix therefore form a thin separating boundary layer with an electric current. In two adjacent regions, the particle populations are frozen to their respective magnetic field lines being prevented from mixing. Due to opposite directions of contacted magnetic fields and external forces pushing plasmas closer, the frozen–in assumption breaks down resulting in a change of magnetic topology. Because the newly reconnected field lines are highly bent, the magnetic tension force heats and accelerates the plasma at high speed. A sketch of the different phases of the process is documented in Figure 2.4.

Depending on the length of the X-line that exists at the center of the diffusion region and the time-scale of the process that breaks the frozen-in condition, magnetopause reconnection may be large scale and quasi-stationary, or patchy and transient.

The concept of magnetic reconnection was introduced in the context of magnetospheric physics by *Dungey* (1961). Since the IMF observed near Earth varies frequently, the magnetosheath magnetic field also varies. Thus, there is always a region at the magnetopause where the magnetosheath and magnetospheric magnetic fields have antiparallel components, and reconnection may occur. The reconnection rate strongly depends on the shear angle and exhibits a sharp peak near 180° (*Anderson and Fuselier*, 1993) that leads to an open magnetosphere.

When IMF points southward, reconnection could occur between the magnetosheath and magnetospheric magnetic fields near the subsolar point (Figure 2.5a).

Newly opened field lines are dragged tailward by two effects: the solar wind flow and the $\mathbf{j} \times \mathbf{B}$ force which act to straighten the highly kinked field lines. More evidence for magnetic reconnection at the subsolar magnetopause under southward interplanetary magnetic field has been found from *in situ* observations reported by (*Sonnerup et al.*, 1981, *Gosling et al.*, 1982). Sudden plasma flow enhancements tangential to the nominal magnetopause surface and much larger than neighboring flows exterior or interior to the magnetosphere are in-

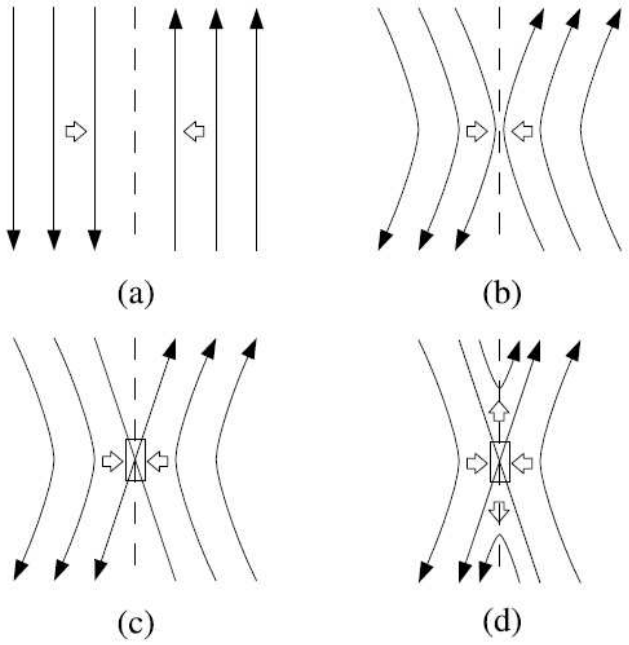

Figure 2.4: A sketch of the different phases of magnetic field reconnection.

dicative of reconnection. It was proposed that dayside reconnection produces a boundary layer of mixed magnetospheric and magnetosheath particle populations by allowing direct plasma entry across the open portion of the magnetopause. The magnetosheath plasma is often accelerated at the magnetopause to speeds greater than those in the adjacent magnetosheath and populate the LLBL (*Paschmann et al.*, 1986). Time-of-flight effects on recently reconnected field lines are expected to cause separation of electron and ion edges of the LLBL with the electron edge earthward of the ion edge (*Gosling et al.*, 1990). It was believed that the LLBL is considered to be predominantly on open field lines for southward IMF (*Luhmann et al.*, 1984).

Dungey (1963) proposed that reconnection may also occur when the IMF is northward. In this scenario, the magnetosheath and magnetospheric magnetic fields are oppositely directed at the magnetopause tailward of the cusp. Such reconnection is usually called high-latitude reconnection. Since the conditions in both hemispheres are equivalent, two conjugated reconnection sites are indicated (see Figure 2.5b). Reconnection takes place not only around the cusp but at a whole dayside part of antiparallel line and thus we can observe the open LLBL covering entirely the whole dayside magnetopause. Evidence for such single lobe reconnection was provided by *Fuselier et al.* (1995), *Milan et al.* (2000), and *Frey et al.* (2002). However, such line can one more time reconnect at the second hemisphere and one would observe the LLBL plasma on closed field lines. This scenario of dual lobe reconnection may occur under strong northward IMF and was described by *Reiff* (1984), *Song and Russell* (1992) and *Song et al.* (2002) (Figure 2.5c). These newly reclosed field lines will sink into the magne-

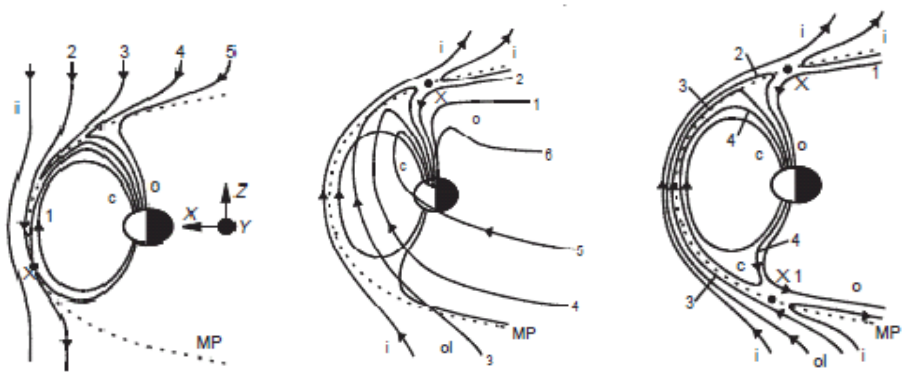

(a) (b) (c)

Figure 2.5: Schematic illustrations of the evolution of reconnected field lines in the magnetosphere (dusk flank view). (a) is for southward IMF whereas (b) and (c) are two of the possibilities for northward IMF in all cases with $B_Y \gg 0$. Field lines and regions are denoted as i - interplanetary field line, o - open field line, c - closed field line, ol - overdraped lobe field line (adapted from *Lockwood and Moen* (1999)).

tosphere and due to the interchange instability will move antisunward around the flanks, thus form a thick LLBL and cold dense plasma sheet (*Øieroset et al.*, 2005). All physically possible reconnection geometries during northward IMF were described by *Cowley* (1973) and include single lobe reconnection, dual lobe reconnection, and sequential merging. The sequential merging process is similar to dual lobe reconnection; however, reconnection processes at both hemispheres do not occur simultaneously.

One of the controversial issues regarding magnetic reconnection at the magnetopause is the location of the reconnection line on the dayside magnetopause during a strong IMF B_Y. There are two hypotheses of where reconnection may occur as a function of B_Y. The antiparallel merging model (*Crooker*, 1979) predicts that reconnection would occur where there is maximum of the magnetic shear across the boundary separating two disparate plasma regimes and predicts no reconnection in the subsolar region when the IMF B_Y (the so-called guide field) is large. The regions extend from near the equator on the magnetopause dawn-dusk flanks up to the cusp regions at local noon. In contrast, the component merging model (*Gonzalez and Mozer*, 1974) predicts that a tilted reconnection line passes through or near the subsolar point irrespective to the value of the IMF B_Y component, so long as B_Z is negative. The differences between these two hypotheses are illustrated in Figure 2.6.

The LLBL formation under dominant B_Y IMF was described in *Němeček et al.* (2003) and it is depicted in Figure 2.7. The figure presents the situation when the magnetosheath magnetic field points duskward above the cusps. Green dots (see Figure 2.7) show the cites with antiparallel fields duskward of the cusp

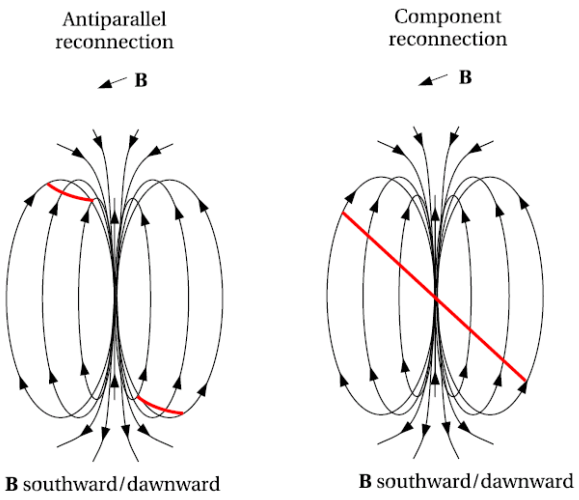

Figure 2.6: Antiparallel (a) and component (b) reconnections.

in the northern hemisphere and dawnward of the southern cusp. In case of small tilt of the Earth dipole, one can expect equal reconnection rate at both hemispheres. In the northern hemisphere the reconnected line is divided into two parts, where one part points duskward of the northern cusp and creates an ionospheric projection of the LLBL and the second part of the reconnected field line ends duskward of the southern cusp and supplies the LLBL precipitation in this region. Since the same reconnection processes occur in the southern hemisphere as well, there are two spots of the LLBL precipitation in both hemispheres. A statistical study (*Merka et al.*, 2002) confirmed that the probability of an observation of the cusp-like (LLBL) plasma peaks at two locations separated in magnetic local time.

2.3.2 Kelvin-Helmholtz Instability

The other candidate mechanism for the LLBL formation involves large-scale waves at the magnetopause. The magnetopause layer is continuously in motion due to the temporal variations in the solar dynamic pressure. This boundary motion can induce wide band of the surface waves from large-amplitude to small-scale waves or ripples. First suggested by *Dungey* (1955), the Kelvin-Helmholtz instability (KHI) may also produce surface waves propagating along the magnetopause. The KHI is hydrodynamic instability that grows in a velocity shear layers. The KHI occurs as well in MHD where a strong magnetic field through their tension stabilizes the instability. The magnetic field perpendicular to the flow tends to demensionalize the dynamics onto the plane perpendicular to the magnetic field (*Nakamura et al.*, 2004). The magnetopause is ideal location for the development of KHIs since it is a thin boundary with considerable velocity shear where the magnetosheath flow is fast relative to the stagnant magnetic plasma population (*Miura*, 1984). *Chandrasekhar* (1981) and *Drazin* (1981)

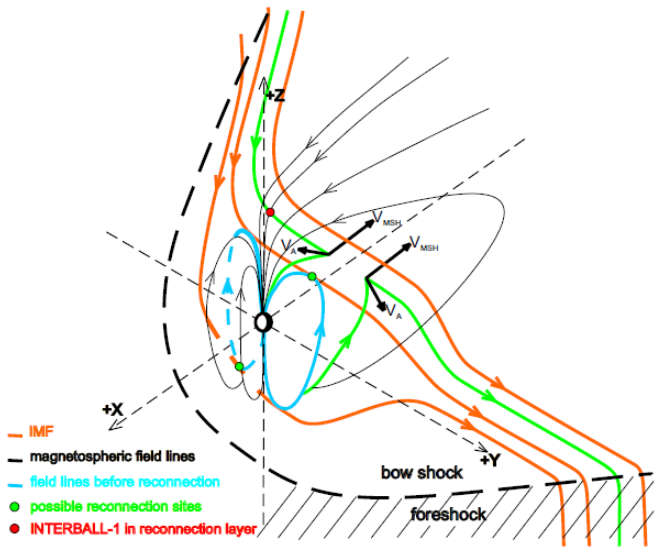

Figure 2.7: A 3-D sketch of the magnetic field lines formed by reconnection duskward of the northern cusp (adapted from *Němeček et al.* (2003))

considered the basic linear theory of the KHI in detail. More recent theoretical achievements in the KHI theory have been summarized in *Fitzenreiter and Ogilvie* (1995) and *Scholer and Treumann* (1997).

The KHI is a suitable subject for computer simulation. MHD equations are derived by assuming that the dynamics at smaller ion and electron scales do not crucially effect the dynamics at the MHD scale (*Nakamura et al.*, 2004). In the simplest linear MHD description, the onset condition for the KHI in an ideal incompressible plasma under assumptions of a discontinuous velocity shear and infinitely thin layer, is

$$[\mathbf{k}\cdot(\mathbf{V_1}-\mathbf{V_2})]^2 > \frac{n_1+n_2}{\mu_0 m_p n_1 n_1}[(\mathbf{k}\cdot\mathbf{B_1})^2+(\mathbf{k}\cdot\mathbf{B_2})^2], \tag{2.5}$$

where the indices 1 and 2 corespond to the two plasma environments on either side of the boundary, n is the plasma number density, m_p the proton mass, m_0 the permeability of free space, $\mathbf{V}$ is the plasma flow velocity, $\mathbf{B}$ the magnetic field vector and $\mathbf{k}$ the wave vector; $\mathbf{V}$, $\mathbf{B}$ and $\mathbf{k}$ are all tangential to the layer. KH waves are caused by a velocity gradient or shear, $|\ \mathbf{V_1}-\mathbf{V_2}\ |$, between the streaming magnetosheath and relatively stagnant magnetospheric plasmas, in the case of the magnetopause.

Traditional KHI surface wave (small-amplitude KH vortices and ripples) does not transport mass across the magnetopause. Numerical simulation models (*Fujimoto and Terasawa*, 1994, *Nykyri and Otto*, 2001, *Nakamura et al.*, 2004) suggest that such transport across the magnetopause can be induced by the KHI only when the KHI has grown sufficiently with formation of the rolled-up vortices. The rolled-up vortices are filled by engulf plasma from either sides of the

magnetopause.

The KHI has been extensively studied via ground observations (*Lee and Olson*, 1980) as well as *in situ* satellite observations (*Fairfield et al.*, 2000, *Nykyri et al.*, 2003). Single spacecraft determination of the wave features such as wavelength, amplitude, propagation velocity is complicated and quite uncertain because such measurements do not allow us to separate normal motion of the magnetopause from tangential wave motion (*Trussoni et al.*, 1982) as well as unambiguously tell whether the KHI can reach its nonlinear stage to generate rolled-up vortices.

A new class of analysis techniques for boundary wave study, empirical reconstruction methods, was proposed by *De Keyser et al.* (2002) that is an attempt to interpret *in situ* observations in terms of stationary structures that are convected across the spacecraft. Continuously changing position of the boundary is considered an unknown variable. Once the motion of the boundary is found, empirical reconstruction produces spatial maps showing how physical quantities vary as a function of the position relative to the boundary.

The multipoint observations at the dusk flank magnetopause have been reported by *Hasegawa et al.* (2004). The authors demonstrated the non-linear rolled-up nature of the vortices with the length scale of one vortex to be 40000-50000 km (Figure 2.9). However, they didn't observe signatures of reconnection. In their MHD simulation *Otto and Fairfield* (2000) pointed out that reconnection can occur inside the narrow current layer generated by the KHI at the flank magnetopause. *Nykyri and Otto* (2001, 2004) quantified this reconnection process inside the KH vortices. According to MHD simulation results, reconnection inside the KH vortices can transport plasma of solar wind origin into the magnetosphere with a transport velocity of $\sim$1.5 km/s. This corresponds to a diffusion coefficient of order 10^9 m^2/s which is sufficient to produce the LLBL at the flank of the magnetopause during northward IMF conditions.

Detailed comparison of measurements based on Cluster observations with 2-D MHD simulations demonstrated by *Nykyri et al.* (2006) indicates that localized reconnection can happen inside the plasma vortices. The most recent study (*Taylor et al.*, 2008) provided the evidence of the simultaneous occurrence of high-latitude reconnection in both hemispheres together with the plasma transport processes at the flank magnetopause induced by the KHI.

However, microscopic dynamics has a strong effect on plasma mixing driven

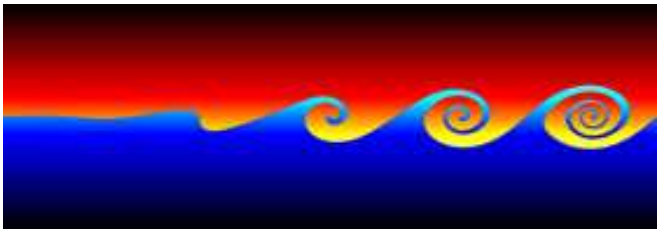

Figure 2.8: An evolution of the Kelvin-Helmholtz instability (from internet).

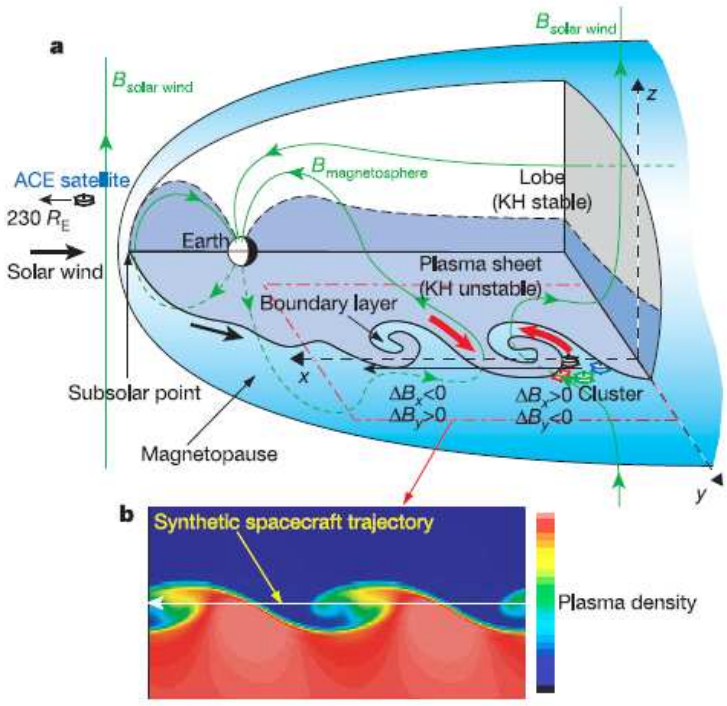

Figure 2.9: (a) A Sketch of 3-D cutaway view of Earths magnetosphere showing signatures of Kelvin- Helmholtz instability. (b) Vortex structure resulting from a 3-D numerical simulation of the KHI. Colour-coded is the plasma density in an x-y cross section cut below the equatorial plane. The density, velocity, and magnetic field variations predicted when a synthetic satellite passes through the centre of the KH vortices (from *Hasegawa et al.* (2004)).

by the KHI. *Fujimoto and Terasawa* (1995) showed that ion mixing across the shear layer during the KH unstable magnetopause was reduced when the background magnetic field is inhomogeneous. Thus, the influence of the instability on the formation of the LLBL may not be as efficient as it seems firstly. Moreover, the KHI occurs at he flanks of the magnetosphere, thus the process cannot explain the observations of the LLBL near the subsolar magnetopause.

2.3.3 Diffusion

Diffusion is one of the basic transport processes in an inhomogeneous medium. Because the magnetopause is a current layer with the density, temperature, magnetic field, and flow gradients, plasma diffusion processes at the magnetopause can contribute to the plasma transfer across the boundary layer (*Eastman and Hones*, 1979). Such mechanisms of the diffusive plasma mixing can explain smooth and gradual density profiles across the LLBL, so that different kinds of a small scale turbulences reduce spatial density variations within the boundary layer. Increasing of the LLBL thickness along the magnetopause with the

increasing distance from the subsolar point also consistent with continuous diffusive plasma entry.

The diffusive velocity is determined by the diffusion tensor $D = (D_\perp, D_\perp, D_\parallel)$, whose components are the diffusivities parallel and perpendicular to the magnetic field. The diffusivity is defined as the ratio of the square of the thermal velocity and the collision frequency: $D = v_{th}^2/\nu$. For a magnetized plasma, the diffusion coefficient is given by (*Ichimaru*, 1973):

$$D_\perp = \rho_e^2 \nu (1 + \frac{T_i}{T_e}), \tag{2.6}$$

where ν is the collision frequency, ρ_e is the electron gyro-radius, T_i (T_e) is ion (electron) temperature.

Classical diffusivity is irrelevant for the LLBL formation because the characteristic free paths of the particles are much more larger than the width of the boundary layer. Since the plasma in the magnetopause region is essentially collisionless, the diffusion must result from anomalous transport process. A strong particle scattering that is necessary for cross-field diffusion, requires a distortion of particle orbits. In the absence of actual particle collisions in the magnetospheric plasma, the distortion of the particle orbits can be provided through wave particle interactions. So in a context of collisionless plasmas, we speak about anomalous resistive diffusion. The influence of cross-field diffusion of the cold magnetosheath plasma into the LLBL becomes more sufficient when the plasma transport through magnetic reconnection (*e.g.*, under northward IMF condition) could be neglected.

Shapiro et al. (1994) reexamined the role of low–hybrid waves at the magnetopause, their interaction with plasma may lead to localized field structure and enhanced diffusion rates exceeding the rate estimated by *Sonnerup* (1980). However, in general, the diffusion coefficients are not high enough to explain the formation of the LLBL (*Treumann et al.*, 1995). *Bauer et al.* (2001) estimated the diffusion caused by lower hybrid drift instability, gyro-resonant pitch angle scattering and kinetic Alfven wave turbulence and suggested that cross-field diffusion cannot transport solar wind plasma into the outer and inner boundary layers at a rate that would account for their thicknesses. It was pointed out that the diffusion process cannot explain the outer boundary layer formation where the density plateau is observed, as it predicts gradient regions only. Other mechanisms which can be responsible for the formation of the boundary layer are curvature drift, gradient B drift, and polarization drift, which must always contribute to the formation of the boundary layer to some degree.

We can conclude that none of the electrostatic turbulent modes may, under normal conditions, build up the inner LLBL by a purely diffusive process based on resistive diffusivities. High diffusivities occur only sporadically and are marginally able to fill the boundary layer.

2.3.4 Impulsive Penetration

Lemaire and Roth (1978) firstly proposed that solar wind irregularities contain-

ing excess momentum can penetrating impulsively through the magnetopause into the Earth's magnetosphere. At the edge of the plasmoid, in the direction perpendicular to the magnetic field and plasma velocity, a polarization electric field is induced which leads to a $\mathbf{E} \times \mathbf{B}$ drift. Later, *Lundin et al.* (2003) provided evidence of this mechanism, which suggests that the transportation of solar wind plasma through the magnetopause releasing via magnetosheath plasma blobs or plasmoids. The mentioned mechanism can explain a simultaneous presence of magnetosheath and magnetospheric populations on the same magnetic field line. It requires the presence of low-energy plasma structures detached from the magnetopause and such negative density gradients when the satellite deeper in the LLBL observes a higher density than the satellite at the magnetopause. However, it is difficult to distinguish the products of impulsive penetration from pressure pulses modulating the magnetopause surface. A survey of two-point magnetopause observations from *Sibeck et al.* (2000) did not reveal any such example of negative gradients. It seems that the impulsive penetration does not play a significant role in the LLBL formation and that is rather rare happened process.

2.3.5 Finite Larmor Radius Effects

Typically, the magnetopause thickness is comparable or several times smaller than the ion gyro-radius of the more energetic magnetosheath particles computed by using their mean thermal velocity. Such energetic particles, for which the Larmor radius is greater than the the thickness of the magnetopause current layer or other boundaries in its vicinity could transfer across the magnetopause due to the finite Larmor radius effects and add the magnetosheath plasma to the adjacent LLBL. However, the present general view is that only a small fraction of the particles may enter the LLBL through this process, largely because plasma charge-neutrality has to be preserved.

2.4 Properties of the LLBL

As mentioned the LLBL is a transition layer, where mass, momentum and energy from the solar wind transfer into the magnetospheric system. The existence of the LLBL as the regular magnetospheric boundary was first revealed by ISEE spacecraft more than 30 years ago (*Hones et al.*, 1972, *Eastman et al.*, 1976). This layer can be found at low latitudes on the whole dayside magnetosphere and along magnetospheric flanks (*Akasofu et al.*, 1973). *Eastman et al.* (1996) based on a statistical study showed that the boundary layer was observed in 90 % of the magnetopause crossings. The LLBL properties and dynamics have been a subject of the extensive studies during last few decades (see AGU monograph 133, Earth's Low-Latitude Boundary Layer, 2003).

The thickness of the LLBL is variable; the layer becomes thicker with increasing distance from the subsolar point (*Haerendel et al.*, 1978). Further, LLBL thickness changes from about 0.1 R_E near local noon (*Eastman and Hones*, 1979)

to about 0.6 R_E at the dawn and dusk flanks (*Paschmann et al.*, 1993). *Haerendel et al.* (1978), *Mitchell et al.* (1987) showed that there is some correlation of the LLBL thickness with the IMF orientation, i.e., the LLBL is thicker under northward IMF conditions. However, several examples of a very thick LLBL (up to several R_E have been reported at flank parts of the magnetopause (*Sauvaud et al.*, 1997). The mean LLBL thickness can exceed 1.4 R_E during the intervals of enhanced solar wind dynamic pressure (4-8 nPa) presumably if the solar wind speed is low and density is high (*Šafránková et al.*, 2007). Flux transient events (FTEs) are one of the crucial factors influencing the LLBL thickness as well, the LLBL is considerably thinner shortly after the detection of a FTE than it was during the event (*Hapgood and Lockwood*, 1995). The particle measurements reveal that the LLBL often exhibits complicated substructure and may be divided into several sublayers according to different ratios of magnetosheath and magnetospheric populations and/or the magnetic field topology. We will discuss this topic in the part 6.3.

The spatial structure of the LLBL is of interest since it provides an indication whether diffusion plays a role in the LLBL formation. Despite the fact that the plasma parameters inside the LLBL are highly variable, the plasma density and temperature change usually in antiphase (*Hapgood and Bryant*, 1990, 1992b, *Hapgood and Lockwood*, 1995). Single spacecraft measurements are not able to resolve spatial and temporal changes due to the large and rapid backward and forward motions of the magnetopause and the LLBL. For solving aforementioned problem, the authors introduced the transition parameter technique. Using the transition parameter, it is possible to reorder plasma and field data and remove the effects of the magnetopause and boundary layer motions from the data analysis. Such dependence of the electron (ion) density vs electron (ion) temperature is usually called the N-T plot.

In a statistical study, *Hapgood and Bryant* (1992b) showed that there is a smooth transition between the magnetosphere and magnetosheath states with many points representing plasma states intermediate between two extremes if data are reordered according to the transition parameter. They concluded that within the boundary layer there is a continuous change in the balance of processes controlling the transition between the magnetosheath and magnetosphere. *Sibeck et al.* (2000) analyzed measurements of the Magion-4 and Interball-1 satellite pair in the LLBL and suggested that the inner satellite nearly always observes plasma of a lower density than that located further from the Earth. The authors pointed out that they found several cases where this rule was broken and that all these events were connected with a fast displacement and deformation of the magnetopause.

Chapter 3

Aims of the thesis

As mentioned in the introduction, solar wind conditions play a significant role in a study of magnetopause processes. However, it is mainly a magnetosheath magnetic field that becomes into contact with the magnetopause. For this reason, the thesis is devoted to the influence of magnetosheath parameters on the magnetopause and LLBL formation. We select two key regions around the magnetopause and discuss three close related topics: turbulent structures in high-latitudes as well as in the dayside magnetopause and spatial-temporal variations of the LLBL profile.

In the first part of the thesis, we study the vortex-like structure filled by slow and heated plasma in the outer cusp during periods of positive IMF B_Z. We analyze and compare in detail the observations of two spacecraft, discuss the differences between them and suggest the way of a formation such structure. We statistically verify whether a discussed phenomenon is a regular feature of the high-altitude cusp region. These investigations are based on data from the Interball–1 and Magion–4 project with high–altitude orbits.

Quasiperiodic fluctuations of magnetic field and plasma parameters at the magnetopause are usually attributed to pressure pulses coming from the solar wind, foreshock fluctuations, flux transfer events or surface waves. Since their observable characteristics are similar at the dayside magnetopause, these events are often misinterpreted and the statistical studies are spoiled. Thus, we made several case studies with motivation to elucidate a different nature of particular events observed near the magnetopause and/or within the LLBL. These structures include the magnetopause surface deformation, LLBL thickening, pulsed reconnection, FTEs and others causes.

All these structures disturb spatial profiles of the LLBL. Nevertheless, we use so called n-T plots (ion and/or electron density vs temperature) to precisely determine these profiles under various solar wind conditions, when mainly the influence of IMF B_Z is considered. Both topics, nature of transient events and variations of the LLBL profile solved in the second part of the thesis are based on multipoint observations from five THEMIS spacecraft during their string–of–pearls configuration when the separations among probes were small. For selected events, we use subsequent phase of the THEMIS mission when probes

were simultaneously located in different regions (magnetosheath, LLBL, plasma sheet).

All particular studies use monitoring of the upstream parameters but we compare them with simultaneous magnetosheath observations whenever they available.

Chapter 4

Instrumentation and data processing

A study of magnetospheric regions (*e.g.*, LLBL or cusp) requires multipoint *in situ* spacecraft observations due to the complex character of investigated phenomena and necessity to distinguish spatial-temporal changes. Since the magnetopause region is sensitive to the influence of the solar wind, it is important to take into account upstream conditions. For our analysis, we used data from a conjunction of five THEMIS spacecraft traversing the magnetopause in the equatorial plane that is ideal for the LLBL study, and supplemented them by the measurements from the Wind and ACE spacecraft that were used as solar wind monitors. One part of this thesis considers the global vortex–like structure in the outer cusp. Therefore, we used the data from the Interball project (Interball–1 and Magion–4) due to its suitable orbits.

In this chapter, we provide an introduction to the THEMIS, Wind, ACE, Interbal-1 and Magion-4 spacecraft summarizing overall scientific objectives and spacecraft orbits along with an overview of the instruments on-board.

4.1 THEMIS

THEMIS (Time History of Events and Macroscale Interactions during Substorms) is the fifth NASA's Medium-class Explorer (MIDEX) mission of 5 identical satellites with a dedicated ground-based observatory array. It provides multipoint and multi-instrument observations focused on clarifying still outstanding questions when and where substorms occur and how transfer of solar wind energy to the Earth's magnetosphere releases. THEMIS was launched on February 17, 2007 and the probes were placed on a highly elliptical orbit from Cape Canaveral. Every four days, the THEMIS spacecraft line up within the Earth's magnetotail, collecting unique measurements of plasma and magnetic field parameters.

The primary goal of THEMIS driven the mission design is to determine an origin and evolution of the substorm instability, to solve dilemma which magnetotail process is responsible for a substorm onset: a local current disruption or the interaction of the current sheet with the plasma emanating from recon-

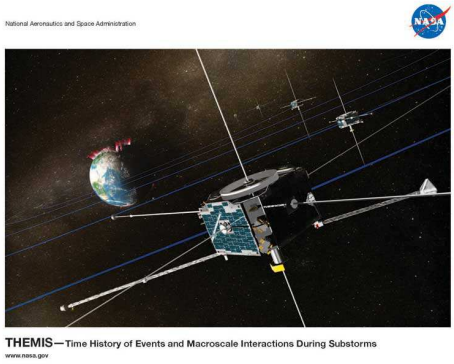

(a)

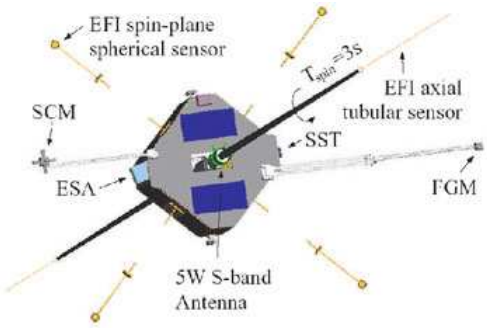

(b)

Figure 4.1: (a) An artist's impression of the THEMIS quintuple, (b) a technical chart (adapted from http://themis.ssl.berkeley.edu/index.shtml).

nection at $\sim$ 25 R_E. However, the probes also traverse the radiation belts and the dayside magnetosphere, allowing THEMIS to address additional objectives. One of the secondary objectives is mechanisms of the radiation belt energization during the recovery phase of storms, production and sources of storm-time MeV electrons. Tertiary objectives of the THEMIS mission concern the solar wind interaction with upstream beams, waves and the bow shock. The mission design and scientific goals are extensively described in these papers: *Angelopoulos* (2008), *Frey et al.* (2008), *Sibeck and Angelopoulos* (2008).

In a period between instrument commissioning and final orbit placement, the THEMIS probes were in a string–of–pearls configuration near their launch orbit (Fig. 4.2). During this interim phase, all five spacecraft aligned in a line crossed the low-latitude magnetopause and the adjacent layers twice a day with short time lags between the spacecraft with the apogee of 15.4 R_E. The distance between the leading and trailing spacecraft was of $\sim$2 R_E, while the separations among inner probes were $\sim$ 1000 km. The string–of–pearls configuration lasted till the middle of September 2007 and covered all dayside magnetopause since apogee rotates from the dusk to dawn side.

In the subsequent phase from the middle of September 2007, the probe positions were re–organised such that the apogee of the orbits were changed to 10, 12, 20 and 30 R_E and moved on the dawn side of the magnetosphere. The apogee rotates slowly around the Earth to cover the dayside, dawnside, nightside, and duskside of the magnetosphere with a corresponding mission phase: Dawn Phase, Tail Science Phase, Radiation Belt Science Phase, Dayside Science Phase. The orbit configurations during the string–of–pearls period and first Dayside Science Phase are shown in Figure 4.2.

During the string-of-pearls configuration and Dayside Science Phase, the THEMIS spacecraft spent many hours at the dayside magnetopause provided observations needed to address unsolved aspects of magnetospheric boundary dynamics. At the dayside the five–probe conjunction allows simultaneous mea-

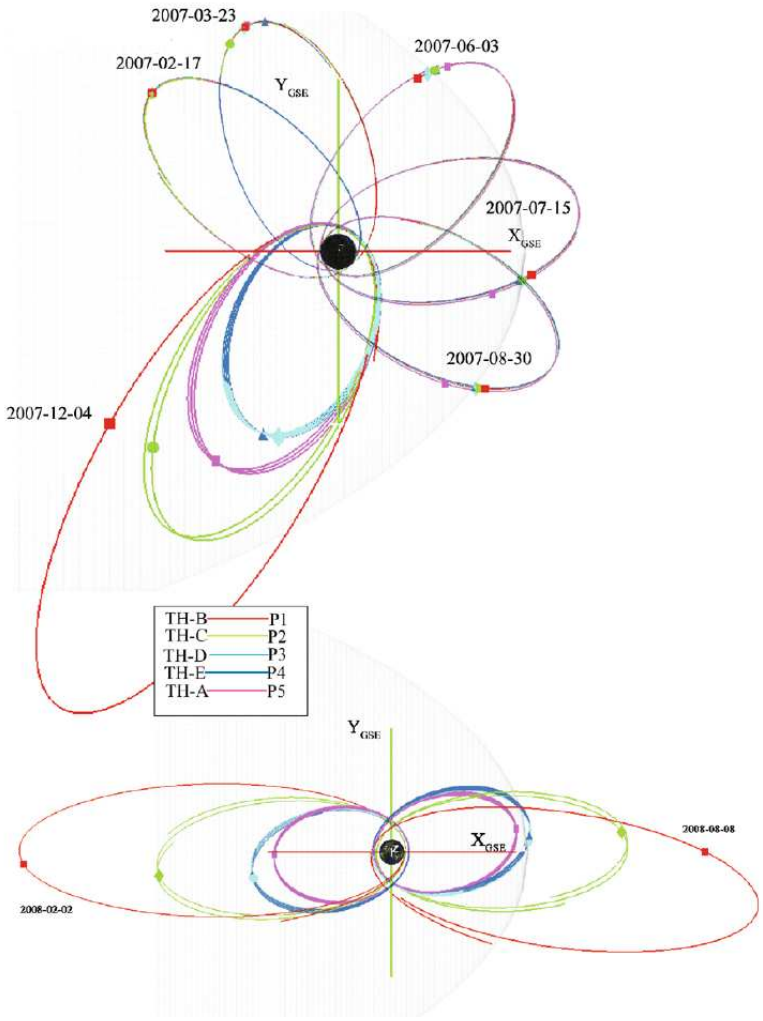

Figure 4.2: THEMIS orbits during the string–of–pearls configuration and first Dayside Science Phase (adapted from *Angelopoulos* (2008)).

surements at the magnetopause, foreshock, and solar wind, offering an opportunity to identify whether the solar wind or foreshock trigger a full range of transient events observed at the bow shock, magnetopause, and in the outer dayside magnetosphere.

Each of the THEMIS spacecraft carries an identical instrumentation including a fluxgate magnetometer (FGM), an electrostatic analyzer (ESA), a solid state telescope (SST), a search coil magnetometer (SCM), and an electric field instrument (EFI). All satellites are spin–stabilized with 3 s spin period.

Fluxgate Magnetometer

Magnetic fields are essential in characterizing different plasma regions in and around the Earth's magnetosphere. Fluxgate magnetometers are the most widely used magnetometers for space applications. FGM (*Auster et al.*, 2008) measures

the background magnetic field and its fluctuations (up to 64 Hz) and is capable to detect variations of the magnetic field within the accuracy of ±0.01 nT. It was particularly designed to study abrupt reconfigurations of the Earth's magnetosphere during the substorm onset phase. The magnetometer is enable to measure magnetic fields in the solar wind, magnetosheath, magnetotail, and outer magnetosphere up to the region dominated by the Earths dipole field so that the instrument operates in a range extended over six orders of magnitude at (±25000 nT). FGM is placed on a 2 m boom and locates on the top of the spacecraft. It consists of a vector compensated three axis fluxgate sensor unit and a mainly digital electronics on a single printed circuit board.

Ion and electron electrostatic analyzers

The plasma instrument is designed to measure the ion and electron distribution functions or, in another words, how many electrons and ions come with a specified energy from a certain direction at a given time. The ion and electron electrostatic analyzers (iESA and eESA) work in an energy range from a few eV up to 30 keV for electrons and 25 keV for ions, respectively (*McFadden et al.*, 2008). The ESA measurements allow us to derive the density, velocity, and temperature of the ambient plasma.

The instrument consists of a pair of top–hat electrostatic analyzers with common 180°×6 fields–of–view that sweep out 4π steradians each 3 s spin period. Particles are detected by microchannel plate detectors and binned into six distributions whose energy, angle, and time resolution depend upon instrument mode. The on–board moment processing includes corrections for spacecraft potential.

Solid-state telescopes

There are two SST instruments on-board provided the measurements of the superthermal part of the ion and electron distributions within the energy range from 25 keV to 6 MeV (*D.Larson*, a personal communication). Each sensor consists of two double-sided telescopes measuring ions on one side and electrons on the other side. The telescopes are arranged side–by–side looking in opposite directions, such that each head is measuring ions and electrons on both sides. Mechanical attenuators diminish the geometric factor within the radiation belts (radial distances from Earth below 8 R_E) by a factor of 100, thereby limiting damage to the silicon detectors from intense fluxes of ions. The telescopes are using for remotely sense the current disruption region and time the arrival of particles energized by reconnection.

Search Coil Magnetometer

SCM measures low–frequency magnetic field fluctuations and waves in three directions and extends the measurements of the FGM from 0.1 Hz to frequencies of 4 kHz (*Roux et al.*, 2008). The SCM is placed at the end of a 1 m boom located at the top of the spacecraft and deployed radialy. The SCM operates

in this range in order to identify the instabilities that trigger substorms. Data from the SCM are especially important for investigation the waves in the current disruption region about 10 R_E in the magnetotail plasma sheet, as well as at larger distances where neutral lines are expected to form.

Electric Field Instrument

EFI measures three components of the ambient electric field (*Bonnell et al.*, 2008). One pair of sensors is deployed to 20 meters, whereas the other pair to 25 meters. Two stiff telescopic booms extend sensors perpendicular to four spinning cables and along the probe's spin axis. Wave measurements cover DC up to 4 kHz, with on–board spectral measurements covering the same ranges, as well as providing an estimate of integrated power in the 100–400 kHz band.

Ground based observations

For the broad coverage of the nightside magnetosphere, an array of stations consisting of 20 all–sky white light imagers and ground magnetometers (when no pre-existing magnetometer is located nearby) covering the Arctic and mid-latitude regions of North America that ensures an accurate determination of substorm onset locations to within 0.5 hours of magnetic local time (*Mende et al.*, 2008). Each white light imager takes auroral images with 3 s resolution.The ground magnetometer records the 3 axis variation of the magnetic field at 2 Hz frequency. Thumbnail images are transmitted in almost real-time from the sites and corresponding overview plots and CDF-data-files are available in two days.

Time resolution

THEMIS instruments have four operation modes: slow/fast survey and particle/wave burst. Throughout most of their orbits, the spacecraft operate in slow survey mode, returning magnetic field vectors, plasma moments, and other parameters with a 3 s time resolution. Near apogee in the magnetotail and in regions of interest like the dayside magnetopause, onboard instruments operate in fast survey mode. In the fast survey mode, FGM samples the magnetic field 16 times per spin, SCM and EFI sample 32 times per spin, and SST and ESA provide observations with greater spatial resolution. Encounters with the bow shock, magnetopause, bursty bulks flows within the magnetotail, magnetic field reconfigurations, and other phenomena trigger burst mode operations. In the burst mode, FGM can sample the magnetic field at up to 128 Hz, while SCM and EFI record the data up to 4096 Hz. Burst mode can be of two types: particle or wave. Particle bursts collect high-resolution distributions and low frequency waveforms. They are aimed at capturing the components of the global magnetospheric substorm instability. Wave bursts are intended to capture the $\mathbf{E} \times \mathbf{B}$ field waveforms of the waves anticipated within a disruption region.

Data Processing

THEMIS has an open data policy and readily provides data, documentation, plots, analysis software. All data are available on three levels: L0, L1, L2. Initially, the raw data files are converted in Level 0 data files. These L0 files are generated as 24 hr files and can already be used directly for data analysis and visualization. The Level 0 files are then converted into Level 1 data files in Common Data Format (CDF). All known anomalies are corrected during this phase of processing. Then follows creature of Level 2 data files that includes calibrated data in physical units and is also available in CDF format. Level 2 data files are created daily and are updated and reprocessed when necessary. Those files do not require further calibration and can be read by any software that is able to access CDF files, such as Fortran, C, Matlab and IDL. The Level 0-2 data products are used to produce Summary Data which are available on the THEMIS website (http://themis.ssl.berkeley.edu/summary.php). THEMIS team also provides a Graphical User Interface (GUI) that allows users quick access to the data and their visualization (http://themis.ssl.berkeley.edu/software.shtml).

NASA's CDAWeb provides THEMIS magnetopause crossing database covered time intervals when individual THEMIS probes were within 4 R_E of the nominal magnetopause, as determined from their orbits and magnetopause model for typical solar wind conditions (http://cdaweb.gsfc.nasa.gov/cgi–bin/gif_walk). For some of our cases, we used reprocessed electron spectra and normalized pitch-angle distributions prepared by *V.Kondratovich*.

For data visualization and data processing, we developed our own programmes written in IDL (Interactive Data Language) that, for example, could display n–T plots (density–temperature dependence) or magnetic field projection on the spacecraft trajectory. Other routines, *e.g.* JOB, were worked up by the staff of Department of Surface and Plasma Science, MFF UK.

4.2 Wind

The Wind spacecraft was launched on November 1, 1994 as a first of two NASA spacecraft in the Global Geospace Science initiative (*Lepping et al.*, 1995, *Ogilvie et al.*, 1995, *Lin et al.*, 1995). Wind, together with Geotail, Polar, SOHO, Interball mission and Cluster constitutes a cooperative scientific satellite project designated the International Solar Terrestrial Physics (ISTP) program that has an object to improve understanding of the solar–terrestrial physics.

The primary science goals of the Wind mission are contribution to the understanding of the static and dynamic properties of the solar wind, investigation of basic plasma processes occurring in the near-Earth space, determination of the magnetospheric output to interplanetary space in the upstream region.

On-board, it has the hot plasma and charged particles Three-Dimensional Plasma analyzer (3DP), the Transient Gamma-Ray Spectrometer (TGRS), the Magnetic Fields Instrument (MFI), the Plasma and Radio Waves (WAVES) experiment, the Solar Wind Experiment (SWE), the Energetic Particle Acceler-

ation, Composition and Transport (EPACT) experiment, the Solar Wind and Suprathermal Ion Composition Studies (SWICS/STICS) experiment and the Gamma Ray Burst Detector (KONUS). A schematic view of the Wind spacecraft is presented in Figure 4.3.

At the beginning, the spacecraft had a lunar swing–by orbit around the Earth. Later in the mission, the Wind spacecraft was inserted into a special "halo" orbit in the solar wind upstream from the Earth, about the sunward Sun-Earth equilibrium point (L1), where the gravitational attraction of the Sun and Earth are equal and opposite. In 1999, Wind executed a number of magnetospheric petal orbits that took it to the rarely sampled geomagnetic high latitudes. Between 2000 and 2002, Wind moved further away from the Sun-earth line reaching 350 R_E. Finally, in 2003, it completed an L2 campaign taking the spacecraft more than 250 R_E downstream of the Earth and 500 R_E downstream of ACE to investigate the solar wind evolution and magnetotail phenomena. Since 2004, Wind has remained at the L1 point.

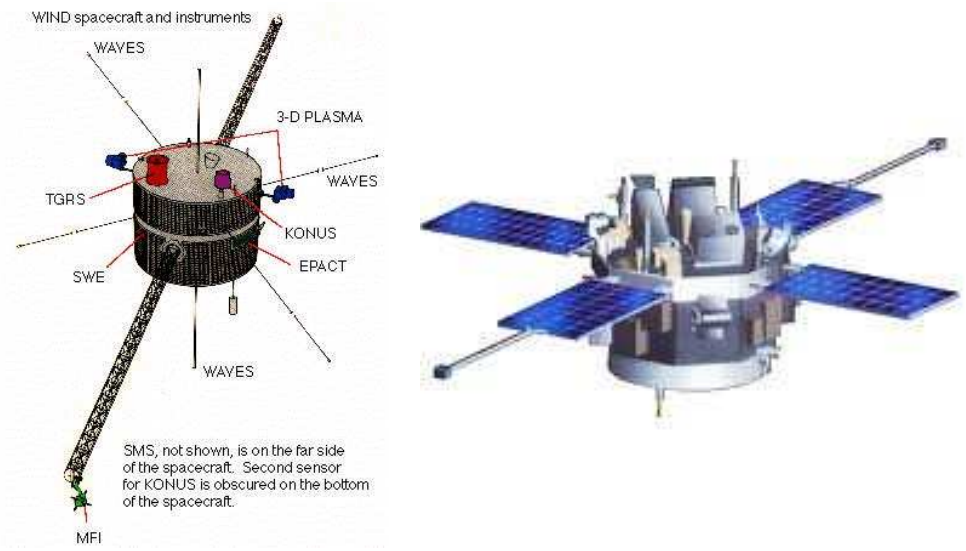

(a) (b)

Figure 4.3: Schematic view of the Wind (a) and ACE (b) spacecraft.

In our analysis, we used Wind as a solar wind monitor and utilized magnetic field measurements provided by the MFI instrument (*Lepping et al.*, 1995) and plasma measurements of the 3DP analyzer (*Lin et al.*, 1995).

4.3 ACE

The Advanced Composition Explorer (ACE) was launched in August 1997 and placed into an orbit near the L1 point. The main goal of ACE is to study particles that come near the Earth from the Sun, from the space between the planets, and from the Milky Way galaxy beyond the solar system. ACE also

traces galactic cosmic rays which come from interstellar space located beyond the heliosphere, but generally from within our galaxy. The ACE spacecraft serves as a space weather station providing a one-hour advance warning of any geomagnetic storms.

ACE has nine instruments onboard that monitor the solar wind and the spacecraft team provides real-time information on solar wind conditions at the spacecraft position. Sensors on ACE are designed to measure the properties of ions from solar wind energies of 100 eV up to several hundred MeV galactic cosmic rays, determining the mass and charge of incident particles during both solar quiet and solar active periods. ACE on-board instruments: Cosmic Ray Isotope Spectrometer (CRIS), Electon, Proton, and Alpha Monitor (EPAM), Magnetometer (MAG), Solar Energetic Particle Ionic Charge Analyzer (SEPICA), Solar Isotope Spectrometer (SIS), Solar Wind Electon, Proton, and Alpha Monitor (SWEPAM), Solar Wind Ionic Charge Spectrometer (SWICS), Solar Wind Ion Mass Spectrometer (SWIMS), Ultra Low Energy Isotope Spectrometer (ULEIS).

The ACE spacecraft is an important addition to current projects including Cluster, THEMIS, STEREO, *etc.* We used ACE as well as Wind for solar wind monitoring and analyze data from MAG (*Smith et al.*, 1998) and SWEPAM (*McComas et al.*, 1998) instruments.

4.4 OMNI

The OMNI 2 database is the hourly and 1 min mean values of the interplanetary magnetic field and solar wind plasma parameters measured by various spacecraft near the Earth's orbit (*King and Papitashvili*, 2005). The data set also contains hourly fluxes of energetic protons, geomagnetic activity indices (AE, Dst, K_P) and sunspot numbers. The OMNI data set is available at http://omniweb.gsfc.nasa.gov/. At the time of studied events presented in this thesis, OMNI data was composed of the Wind and ACE spacecraft measurements, both located at the L1 point. OMNI data were used for the analysis of the upstream conditions and were compared with data from other spacecraft in order to find the optimal solar wind monitor.

4.5 Interball-1, Magion-4

Interball was a multi-national project consisted of two pairs of spacecraft. It was managed by the Russian space agency (RKA) in the framework of a wide international cooperation. Two main spacecraft of the Prognoz series were made in Russia, each with a small subsatellite (Magion) that was made in former Czechoslovakia. Figure 4.4a gives an artist's view of the Interball project. The main objective of this project was to study the physical mechanisms responsible for the transmission of solar wind energy to the magnetosphere, its storage there, and subsequent dissipation in the tail and auroral regions. Interball-1 (the Tail Probe) and a sub-satellite (MAGION-4) were launched in August 1995 into

highly elliptical orbits with a period of 92 h, an apogee of about 190000 km, and an inclination of 62.8°.

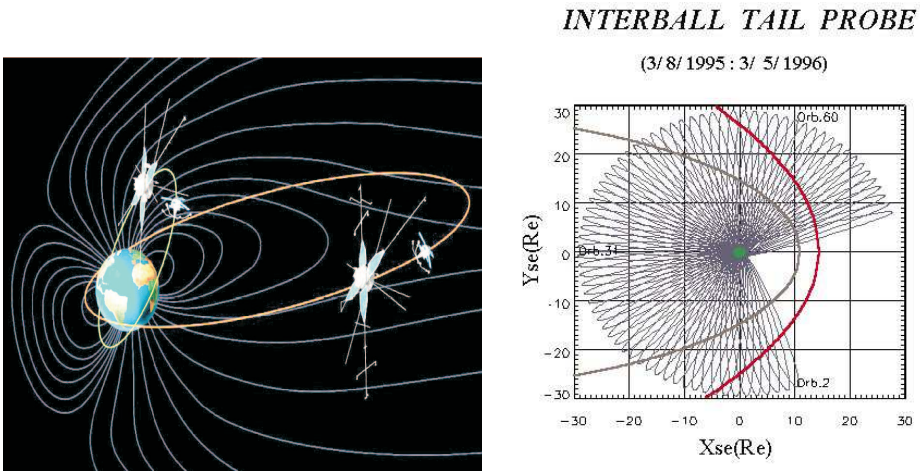

(a) (b)

Figure 4.4: (a) An artist's view of the Interball mission. (b) Interball-1 orbit during first year.

The main spacecraft had more than twenty scientific instruments. The spacecraft was cylindrical, with spin axis toward the sun (within 10°), and with spin period of $\sim$ 120 s. The electric and magnetic field sensors were placed on booms connected to the ends of the solar panels. The subsatellite was small with about ten scientific instruments. The spin axis was directed within 10° of the Sun direction, with a spin period of $\sim$ 120 s.

The Interball–1 and Magion–4 orbits were particularly suitable for solar wind/magnetosheath and magnetospheric substorm studies. Two-point measurements allow us to distinguish reliably the locations and motions of various plasma structures and inhomogeneities. The orbital characteristics have been optimized in such a way that Interball-1 crossed the neutral sheet of the magnetotail in the distance range of $\sim$8–20 R_E from the Earth (Figure 4.4b). Separation distances were ranged from hundreds of kilometers to several tens of thousands of kilometers for the Tail Probe pair and were adjusted according to the physical processes under study, *e.i.*, the distance was increased during tail passages and usually reduced for magnetopause and bow-shock studies at the dayside. Since the orbits were inclined to $\sim$ 62°, the spacecraft often scanned the vertical profile of the cusp region from middle altitudes toward the magnetopause (*Sandahl et al.*, 1997).

The magnetic field measurements on-board Interball–1 spacecraft were carried out by MIF-M and FM-3I instruments (*Klimov et al.*, 1997). FM-3I consists of two fluxgate magnetometers M1 and M2 operated in to different ranges, $\pm$200 nT and $\pm$1000 nT, respectively. The M2 magnetometer was mainly dedicated for attitude control of the Interbal-1 location. The time resolution of both mag-

netometers was 16 Hz. The fluxgate sensors of MIF-M instruments consist of three identical fluxgate core rings, forming a right orthogonal system with fixed orientation with respect to the spacecraft body. They are mounted on the end of the boom of 11 m long. They form the second, in addition to the FM-3I experiment, dual magnetometer system. MIF-M operation range was from 0.3 to 37.5 nT with frequency of 0–2 Hz.

The omnidirectional plasma sensor VDP was designed to determine the integral flux vector and the integral energetic spectrum of ions and electrons in the energy range of 0.2–2.4 keV (*Šafránková et al.*, 1997). For simultaneous measurements in all directions, the VDP device is equipped with six Faraday's cups (FCs) so that their axes formed a three dimensional orthogonal system. The configuration of the VDP detectors was sufficient for determination of flow directions even in highly turbulent regions. The maximum data resolution was 16 samples per second.

The ELECTRON instrument measured electron distribution functions in the energy range from 10 eV to 26 keV in a satellite rotation period (*Sauvaud et al.*, 1997). ELECTRON selected incoming electrons according to their energy by electrostatic deflection in a symmetrical hemispherical analyser having a uniform angle–energy response and detects them with two microchannel plates and discrete anodes. This instrument did not operate through the radiation belt.

Energetic particles were registered by the DOK-2 instrument (*Kudela et al.*, 2002) that consisted of narrow surface-barrier silicon detectors measured ion (20-–850 keV) and electron (25–400 keV) energetic spectra.

Due to the reduced available mass and power allocations on–board the MAGION-4 subsatellite, experiments have been made as simple as possible to fulfill their scientific objectives. The set of MAGION-4 detectors provided measurements of all basic plasma and magnetic field parameters which can be compared with more complex measurements taken onboard the main INTERBALL-1 satellite (*Zelenyi and Sauvaud*, 1997, *Nemecek et al.*, 1997).

The MAGION-4 satellite composed of 10 instruments but in a framework of this thesis, we used data from the plasma flow detector VDP–S, electron and proton spectrometer MPS/SPS, three-component magnetometer SGR and energetic electron and proton spectrometer DOK-S.

Chapter 5

High-altitude Cusp

The existence of the Earth's magnetospheric cusps originally was proposed in *Chapman and Ferraro* (1931) magnetosphere model. The cusp has traditionally been described as a narrow funnel-shaped region in both hemispheres where the Earth's magnetic field lines are directly interconnected with the interplanetary magnetic field lines and shocked solar wind in the magnetosheath has a direct access to the magnetosphere. Reconnection produces accelerated plasma populations which excite different kinds of plasma waves. As a result, the region adjacent to the magnetopause is highly turbulent and occupied by the heated magnetosheath-like plasma with a low drift velocity. This region is called the turbulent boundary layer, stagnation region or exterior cusp in different papers (*e.g.*, *Haerendel et al.*, 1978, *Paschmann et al.*, 1978) and it seems to be a proper source of the cusp precipitation.

The numerous low-altitude orbiting spacecraft and ground-based measurements provided precise characterization of cusp's plasma properties and its global motion in response to dynamic changes in upstream and magnetospheric parameters. The cusp-like plasma was found in range 73°-80° MLAT and 10.5-13.5 h in MLT (*Newell et al.*, 1989). High-altitude measurements made by past and present missions such as Interball, Polar, IMAGE, Cluster revealed that cusp definition as a narrow region near the local noon is too confined, it covers a larger portion of the dayside magnetosphere (*Němeček et al.*, 2004) and the cusp diamagnetic cavity filled by charged particles with energies from 20 keV up to 10 MeV (*Chen and Fritz*, 2005).

The interconnection of IMF with the Earth's magnetic field has a dominant effect on the magnetosphere and ionosphere, as a mechanism for both plasma and energy inputs from the solar wind. Present observational facts show that magnetic reconnection is a dominant source of the cusp plasma, whereas other mechanisms can contribute to the cusp population under specific circumstances. The cusp magnetic field reversal topology permits southward and northward IMF to reconnect with the Earth's magnetic field. For southward IMF, reconnection takes place at the subsolar magnetopause and the cusp region is influenced by the reconnection outflow driven by the swept tailward magnetic field lines. For northward IMF, the reconnection process could happen poleward of the cusp

with a sunward convection flow driven by open field lines moving equatorward through the cusp.

The outer boundary of the exterior cusp is confined by the free-flow stream lines of the magnetosheath flow and the inner boundary by the magnetopause indentation (*Lavraud et al.*, 2004b). Such indentation results from the pressure balance at the magnetopause (*e.g.*, *Sotirelis and Meng*, 1999) because the magnetic field exhibits minima at cusps (*Cargill et al.*, 2004). The indentation was predicted by *Spreiter and Briggs* (1962) and later detected by the different spacecraft, HEOS–2, ISEE, Hawkeye, Interball–1, Magion–4 (*e.g.*, *Rosenbauer et al.*, 1975, *Petrinec and Russell*, 1995, *Němeček et al.*, 2000). Recently, *Šafránková et al.* (2002b) suggested and *Šafránková et al.* (2005) confirmed the presence of a magnetopause indentation in the cusp region. *Zhang et al.* (2007) have analyzed Cluster observations, both statistically and for individual crossing cases, and concluded that the boundary between the magnetosheath and cusp seems to be indented in the XY plane and it is less clearly indented in the XZ plane. This indentation can slow down the magnetosheath flow (*Němeček et al.*, 2007). Some other aspects of the magnetopause indentation and outer cusp region were discussed in *Lavraud et al.* (2004a,b).

There is a volume above the magnetopause (encircled in Fig. 5.1) that would exhibit a different plasma behavior than the free-flow magnetosheath. *Sotirelis and Meng* (1999) suggested a secondary stagnation point in this region when the magnetic dipole is tilted toward the Sun in a particular hemisphere and *Haerendel et al.* (1978) argued that the whole volume would be filled with a stagnant plasma. The knowledge of the plasma parameters in this volume is very important because the plasma there supplies the cusp during periods of the northward IMF. Unfortunately, this region is visited by the spacecraft rather rarely and thus there are only a few studies dealing with the plasma flow and magnetic field just above the cusp (*Němeček et al.*, 2003, *Bogdanova et al.*, 2005, *Panov et al.*, 2008).

As it was stressed out, the exterior cusp is a highly turbulent region filled by hot and stagnant plasma for which an occurrence of vortices is a very common feature (*Savin et al.*, 1998, *Alexandrova et al.*, 2006). During a period of positive IMF B_Z, *Šafránková et al.* (2002a), *Merka et al.* (2005) have discussed a vortex–like cavity filled by slow-moving heated plasma inside the outer cusp. However, both papers leave this interesting event without an explanation. In A1 (***Tkachenko** et al.*, 2008b), we present a detailed analysis of this vortex-like structure using the data from Interball-1 and Magion-4, and find necessary conditions and a possible mechanisms to creation of such structures.

The vortex-like structure was observed by both spacecraft on 5 June 1996 between 18:20 and 19:00 UT. The spacecraft moved outward from the magnetosphere and crossed the magnetopause at (2.9; -2.2; 8.7) R_E. We note that both spacecraft cross the magnetopause inside the indentation caused by the depression of the magnetic field; first, Magion–4 at 18:41 UT and then, Interball–1 at 18:51 UT. The temporal separation of the spacecraft was $\sim$540 s.

Solar wind parameters, IMF strength and components are monitored far up-

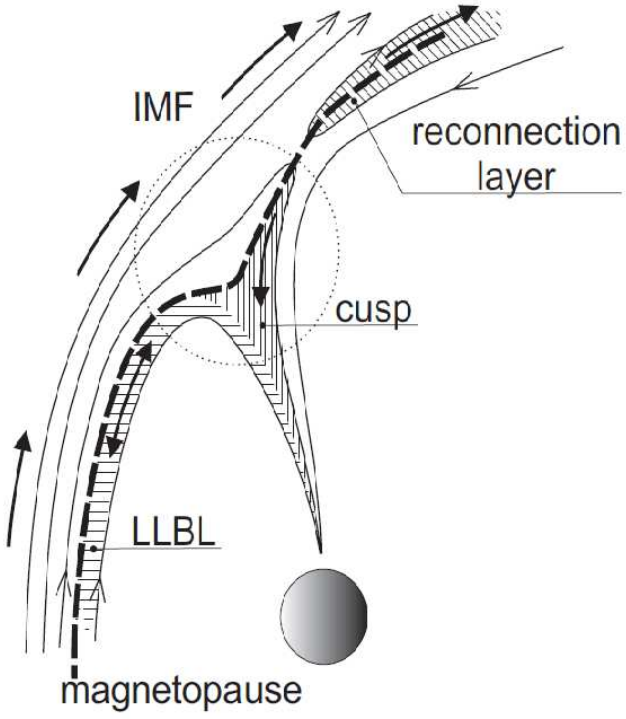

Figure 5.1: The cusp configuration during a prolonged interval of northward pointing IMF. The light lines represent IMF and Earth's magnetic field lines; the heavy arrows show the dominating flow directions in the cusp and adjacent regions. The dotted circle shows the region under study.

stream by Wind (181.0; 6.3; -13.2) R_E in GSM coordinates and close to the bow shock by IMP 8. They showed relatively stable conditions (solar wind dynamic pressure ∼2.7 nPa with the solar wind speed ∼350 km/s and density varying between 9 and 11 cm^{-3}). For our study, it is important that the IMF points generally tailward and northward and the IMF B_Y component is negative or nearly zero during the investigated interval. A small value of IMF B_Y makes the analysis easier because a large B_Y value shifts the reconnection site dawnward/duskward of the cusp proper and the possible inflow from the conjugated hemisphere should be considered (*Němeček et al.*, 2003).

The studied structure was first observed by Magion–4 in the time interval from 18:41:00 to 18:45:30 UT and can be clearly identified in the changes of the magnetic field directions (Fig. 5.2) that exhibit a complicated rotation during the crossing of a thick boundary layer. At the beginning of the interval (until 18:41:30 UT), the measured magnetic field has the magnetospheric orientation and its orientation is magnetosheath-like at the end of the event (18:45:30 UT).

The detail inspection of the spectrograms allows us to divide a whole interval into several parts that are distinguished by the lines and numbers in Fig. 5.2. The comparison of the ion energy spectra measured in antisunward (Ei0) and

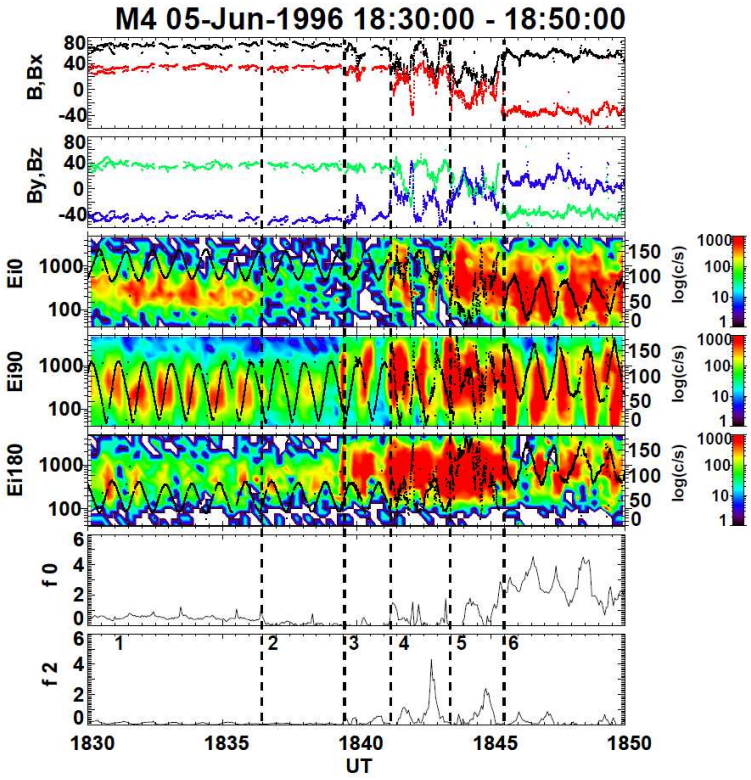

Figure 5.2: Vortex-like structure observed by Magion-4. From top to bottom: the strength and the components of the magnetic field (the GSM coordinate system, B_X - red, B_Y - green, B_Z - blue); spectrograms of tailward (Ei0), perpendicular (Ei90), and sunward (Ei180) streaming ions in the energy range from 100 eV to 25 keV together with their pitch angles (black lines inside the spectrograms) and ion fluxes in units of 10^8 cm^{-2}s^{-1} measured in tailward (f0) and perpendicular (f2) directions. The vertical lines and numbers denote the different regions of plasma populations.

sunward (Ei180) directions shows that the ion flow was oriented sunward at the leading edge of the structure, nearly standing inside, and the tailward flow dominates at the trailing edge. The properties of the plasma and magnetic field inside the numbered intervals are described in ***Tkachenko*** *et al.* (2008b)-A1. The magnetosheath proper was identified by the increase of the tailward flux. Also, we would like to stress out that we have found two magnetic field rotations from magnetospheric to magnetosheath orientations at 18:41 and at 18:45:20 UT, however, only the first of them possesses all attributes of the high-latitude magnetopause.

A similar structure was registered by Interball–1 about 8 min later, between 18:49:00 and 18:56:30 UT. Since both spacecraft moved essentially along the same orbit from the magnetosphere and their separation along the orbit was approximately the same as the time lag between observations of the analyzed

structure, we suggest that the whole region was standing and that the time of observations can be converted into the spatial scale.

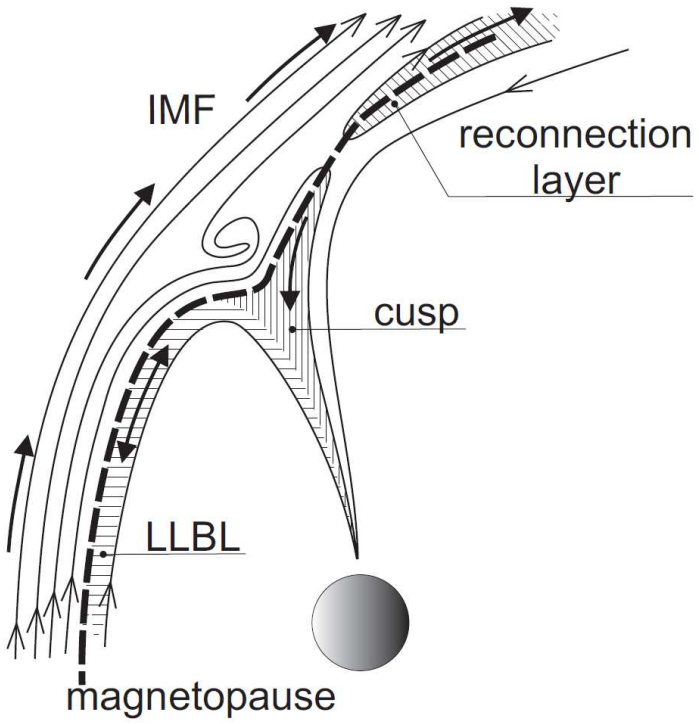

Figure 5.3: A sketch of the high–altitude cusp formation under northward IMF with an illustration of a probable shape of the analyzed structure.

The region 5 observed by Magion–4 and later by Interball–1 is bounded from both sides by the magnetic field rotation from the magnetospheric to magnetosheath orientation. First of them exhibits principal features of a crossing of the high-latitude magnetopause under northward IMF, *i.e.*, high magnetic shear and a presence of the ions accelerated by reconnection proceeding tailward. However, the second magnetic field rotation was observed inside a region of a high density and no reconnection outflow was detected. Although lobe reconnection can be bursty (*Šanfránková et al.*, 1998) and thus, reconnection products can absent, we suggest that the second magnetic field and flow rotations cannot be attributed to the magnetopause crossing but that the spacecraft crosses a structure in the magnetosheath and the direction of the magnetic field is determined by a slow plasma motion. The high temperatures inside this region together with the high plasma density cause a diamagnetic effect. Sharp changes of the magnetic field direction on the edges of this structure and a magnetic field rotation inside that can be clearly identified in spite of a high fluctuation level suggest a vortex-like shape of this structure.

Our understanding of a formation of such structure in the cusp region is presented in Fig. 5.3. This figure repeats Fig. 5.1 with an addition of the magnetic field line rotating consistently with observations. The figure shows

a magnetopause indentation that creates an obstacle to the plasma flow. We assume that when the fast magnetosheath flow encounters the tailward edge of the magnetopause indentation, an eddy is created and the frozen-in magnetic field lines are rolled up. Since the estimated dimension of the eddy is only about 0.25 R_E, it is oversized in Fig. 5.3 for a better readability.

Based on the presented event, we have carried out a limited statistics of the presence of vortex-like structures in the high–altitude cusp region. The results of this half-year period of 1996 statistics are summarized in Table 5.1 that contains solar wind parameters for the events. From these 35 events, we registered vortex-–like structures in four cases. In two events, the IMF B_Z component was positive and through one event, the IMF B_Z turned from positive to negative values (no solar wind monitor was available in one studied case). Unfortunately, our limited statistics does not allow to put ultimate conclusions on solar wind conditions favorable for creation such structures.

	Date	**p** (nPa)	**V_X** (km/s)	**n** (cm^{-3})	**B_Z** (nT)	**Time of event**
1	02.01.1996	3.4	-385	10	+ -	
2	06.01.1996	3	-400	11	-	
3	10.01.1996	2.2	-325	11	-	
4	13.01.1996	2	-400	20	n/a	2100–2130 UT
5	17.01.1996	2.5	-460	6	-	
6	21.01.1996	3	-420	8	+	
7	28.01.1996	3	-395	10	-	
8	01.02.1996	2.5	-425	7	+ -	
9	05.02.1996	1.5	-365	5.5	+	
10	09.02.1996	1.5	-400	5	+	0450–0520 UT
11	16.02.1996	5.4	-365	20	+	
12	20.02.1996	1.6	-500	3	-	
13	02.03.1996	2.5	-310	3	+ -	1950–2030 UT
14	06.03.1996	1.8	-400	6	+	
15	10.03.1996	2.8	-390	9	-	
16	14.03.1996	1.8	-540	3	-	
17	18.03.1996	2.2	-440	5	-	
18	21.03.1996	3	-610	4	+ -	
19	25.03.1996	3	-580	4.4	-	
20	29.03.1996	3.5	-440	8	+	
21	02.04.1996	3.1	-330	14	-	
22	05.04.1996	1.8	-370	7	+	
23	13.04.1996	2.6	-400	8.5	-	
24	21.04.1996	1.8	-550	3	+	
25	24.04.1996	2.4	-395	8	-	
26	28.04.1996	2.2	-400	7	+	
27	13.05.1996	1.8	-500	4	-	
28	17.05.1996	1	-380	3.6	-	
29	21.05.1996	2.6	-430	7.5	-	
30	29.05.1996	1.0	-380	3.6	+	
31	01.06.1996	1.5	-365	3	-	
32	05.06.1996	2.6	-340	11	+	1830–1900 UT
33	09.06.1996	2	-365	8	- +	
34	13.06.1996	2	-335	9	+	
35	17.06.1996	2.2	-380	7.7	- +	

Table 5.1: Statistics of vortex-like structures in the high-altitude cusp region. p - solar wind dynamic pressure; V_X - x-component of solar wind velocity; n - ion density in the solar wind; B_Z - sign of the IMF B_Z component, in some cases we observed changes of IMF B_Z from positive to negative (+ -) or vice versa (- +); Time of event - the time corresponded to the observed vortex-like structure.

Chapter 6

Low–latitude Boundary Layer

6.1 Flux transfer events

Plasma structures at the magnetopause are often signatures of flux transfer events FTEs (*Russell and Elphic*, 1978, *Haerendel et al.*, 1978). They are characterized by a bipolar oscillation in the boundary normal component of the magnetic field (B_N), mixtures of magnetosheath and magnetospheric plasmas, and either enhancements or crater–like variations of the magnetic field strength at the event center. Statistical surveys showed that FTEs are observed predominantly when the magnetosheath or IMF point southward (e.g., *Berchem and Russell*, 1984, *Rijnbeek et al.*, 1984, *Southwood et al.*, 1986, *Kuo et al.*, 1995), strongly suggesting an association with the time–dependent magnetic reconnection process that was proposed as fundamental to the coupling of mass and energy between the solar wind and magnetosphere (*Dungey*, 1961).

The properties and structure of FTEs have been a subject of many studies in the last years, however, a significant progress started with new spacecraft missions as Cluster and THEMIS. For example, Cluster contributed: (1) to discussion of the differences in the signatures between closely separated ($\sim$ 600 km) spacecraft that indicated the substructure of the FTE on this scale (*Owen et al.*, 2001); (2) to a better understanding of the FTE formation and to determine the cross–sectional profiles (*Sonnerup et al.*, 2004, *Fuselier et al.*, 2005, *Hasegawa et al.*, 2006), and (3) to studies of the diffusion region of magnetic reconnection at the magnetopause (e.g., *Vaivads et al.*, 2004, *Retinò et al.*, 2006).

Owen et al. (2008) concentrated on the temporal nature of crater–like FTEs at the dayside high–latitude magnetopause. The authors have reported observations of signatures observed by Cluster that have previously been the source of debate as to whether they are caused by pressure–induced waves on the magnetopause (e.g., *Sibeck*, 1990, 1992) or whether they are the result of encounters with various reconnection boundary layers (e.g., *Smith and Owen*, 1992). They argued that their observations are consistent with reconnected flux tubes created by a transient and localized patch of reconnection located nearer to the subsolar point, moving northward and duskward over three of the four spacecraft. The FTE signatures arise from this transient inward motion of reconnection–

associated boundary layers over the spacecraft.

To contribute to this debate, we analyze a series of FTE-like events observed by THEMIS. We argue that although the event exhibits clear FTE signatures in the magnetic field, the plasma measurements are inconsistent with this interpretation and we assume another mechanism for an explanation of observed phenomenon.

In ***Tkachenko*** *et al.* (2011a)-A2, we analyze observation of the THEMIS spacecraft at the low-latitude magnetopause on August 26, 2007 around 0750 UT. The spacecraft were in string of pearls configuration leaded by THB (9.9; -7.4; -3.7) R_E that was followed by shortly separated THC (9.5; -7.4; -3.6), THD (9.4; -7.5; -3.6) R_E, and THE (9.4; -7.3; -3.6) R_E. The trailing spacecraft, THA (7.9; -7.5; -3.2) R_E, was in the magnetosphere during the event and it did not observe any changes. Upstream conditions were very quiet. The solar wind dynamic pressure measured by ACE and propagated toward the THB location was about 1 nPa and slightly decreased during the investigated interval; IMF was B_Y dominated and the only change was a temporal decrease of the IMF B_Z component to -1 nT between 0746 and 0749 UT.

In spite of the quiet upstream conditions, a lot of activity is observed by THB in the magnetosheath. The magnetic field is much larger than that in the solar wind but its direction is consistent with the IMF draping around the equatorial magnetopause. The B_Y component of the magnetosheath magnetic field is negative and largest component and B_Z turns its sign several times. It starts from positive values and the changes of the sign are about synchronous with the IMF changes at 0746 and 0749 UT.

Transformation of the THEMIS magnetic field in boundary normal coordinates reveals a clear bipolar signature in the THC–THE data and not so clear but still visible bipolar change in the THB data at $\sim$ 0751 UT.

We propose two possible interpretations of the THEMIS observations. First, it is the FTE scenario. The magnetic field behavior is consistent with it because all spacecraft observe bipolar B_N signatures accompanied with the enhancement of the magnetic field strength.

The region of a depressed density corresponds to a region of enhanced magnetic field. A typical dimension of FTE would be about 1 R_E and the duration of observations ($\sim$ 80 s) together with the mean velocity ($\sim$ 100 km/s) lead to a similar value. Consequently, the spacecraft separated by $\sim$ 0.15 R_E can observe very similar changes of the velocity and magnetic field in the magnetosheath, whereas the magnetospheric density is enhanced to nearly magnetosheath value. The flux rope that can produce the described features is shown in Fig. 6.1a. The sketch presents a cross-section in the XZ plane. Such flux rope can be created by a multiple component reconnection along the line of maximum magnetic shear. This process would create a spiral magnetic field inside the flux rope that is shown as closed ellipses in our sketch. In order to meet a majority of observed signatures, we should expect that the rope was created southward of the spacecraft and proceeds northward as the green arrow shows.

On the other hand, there are several features inconsistent with this explana-

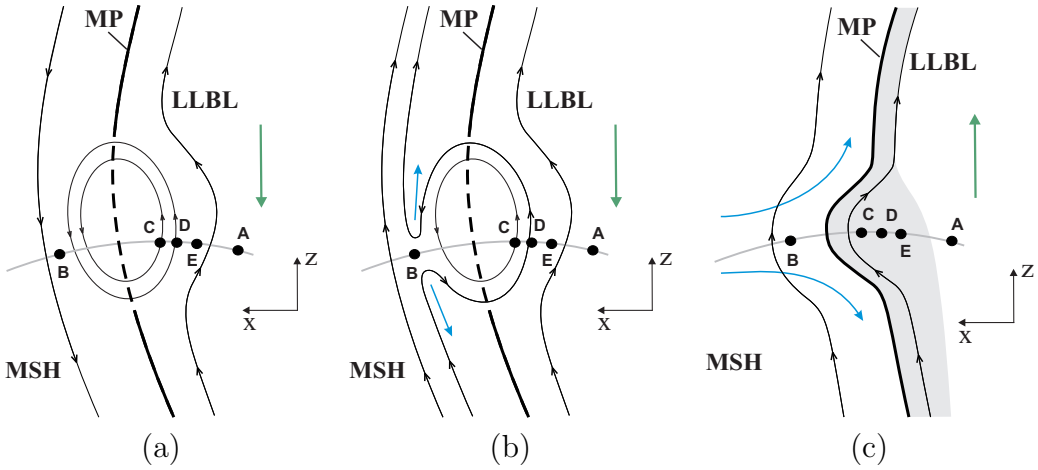

Figure 6.1: A schematic drawing of two possible interpretations of the THEMIS observations. (a) A flux rope created by southward IMF, (b) destruction of the flux rope after an IMF turn to the northward orientation, and (c) interpretation of the observations in terms of a local magnetopause deformation.

tion. First, there are the changes of the v_Z direction observed by THB. We think that these bursts can be associated to the reconnection outflows. If we expect that the flux rope was created during a southward IMF and then it turned northward, the conditions at the fox rope–magnetosheath interface would be favorable for new reconnection that can destroy the original flux rope as it can be seen in Fig. 6.1b. However, the duration of the enhanced plasma flow in THC data is much longer than the duration of the flux rope deduced from the magnetic field observation and this feature contradicts to the interpretation of the event in terms of FTEs.

The second possible scenario is schematically shown in Fig. 6.1c. The bipolar structures in THEMIS magnetic fields are caused by a deformation of the magnetopause connected with the transient decrease of the magnetosheath density that is associated with the turn of the magnetic field. If such bump would proceed northward, it will produce all aforementioned signatures. A nearly continuous enhanced magnetospheric flow is caused by lobe reconnection that builds–up a thick LLBL and the THC-E spacecraft appears in this layer. This idea is supported by a gradual decrease of the magnetospheric magnetic field prior to the event because an increase would be expected for the flux rope scenario.

We would like to point out that if the magnetopause surface would locally follow the changes of the magnetosheath density there will be more than one bump on its surface and it can explain multiple changes of the v_Z sign.

6.2 Structure of the LLBL

An analysis of the LLBL topology revealed that it has a layered structure and could be divided into several sublayers. According to *Song et al.* (1990), the first

sublayer, called the outer boundary layer (OBL), is dominated by magnetosheath particles, and the second sublayer, called the inner boundary layer (IBL), is characterized mainly by the magnetospheric population. Inside the OBL, the plasma density and temperature are almost stable, while across the IBL, the plasma temperature strongly increases. In their observations, plasma inside the different layers is homogeneous and some boundaries exist between two layers suggesting that a little diffusion is present. In an extended study, *Song et al.* (1993) showed that the structure of the LLBL can be even more complicated and that for some examples, a middle boundary layer is present and that slight heating may occur in the boundary layers. In the case of two layers, the ion velocity distribution consists of a simple mixture of two populations whose ratio is systematically changing.

Similar observations of the substructure of the LLBL were presented by *Le et al.* (1996) based on the analysis of ion data. They demonstrated that inside the OBL, a little or no magnetospheric population is observed and only the heated magnetosheath plasma is registered and, on the other hand, inside the IBL, a mixture of magnetosheath and magnetospheric plasma is observed. Also *Vaisberg et al.* (2001) demonstrated that the LLBL may consist of two regions, separated by a thin boundary, and that the number density profile is monotonous across the sharp boundaries. The authors showed that the IBL is occupied by a mixture of both populations and that the trapped magnetospheric population is always observed in the inner LLBL and may also be observed in the outer LLBL. Furthermore, *Bauer et al.* (2001) showed that the plasma in the OBL is dominated by solar wind particles and that the partial densities of the solar wind and magnetospheric particles are comparable inside the IBL. The authors discussed 'warm', counterstreaming electrons that originate predominantly in the magnetosheath and have a field–aligned temperature higher than the electron temperature in the magnetosheath by a factor of 1-5 and that they are characteristic feature of the IBL. Inside the OBL, the density plateau is often observed and the plasma density exhibits step–like profiles inside the outer and inner boundary layers and that the step–like substructure of the LLBL is observed during any IMF orientation.

Following this short survey, it is clear that the IMF orientation controls processes of the LLBL structure and its formation and that magnetic reconnection plays a significant role. Thus, the study of the reconnection topology of the magnetic field lines which populated the LLBL near the dayside magnetopause and the LLBL (cleft)/cusp at low latitudes using multi-spacecraft observations (e.g., *Bogdanova et al.*, 2008) is of the great interest.

Briefly, the LLBL formation on open field lines during a southward IMF is well understood in terms of dayside reconnection (*Dungey*, 1961, *Luhmann et al.*, 1984). Through periods of a strong northward IMF orientation (e.g., *Crooker*, 1979, *Cowley*, 1973), magnetosheath field lines may reconnect poleward of both cusp regions nearly simultaneously and open field lines from both lobes reconnect with a part of the magnetosheath field lines creating newly reclosed field lines with captured magnetosheath plasma (*Reiff*, 1984, *Song and Russell*, 1992, *Song*

et al., 2002) (and the experimental evidences (e.g., *Le et al.*, 1996, *Onsager et al.*, 2001, *Fuselier et al.*, 2002, *Němeček et al.*, 2003)). These newly reclosed field lines may sink into the magnetosphere and move antisunward around the flanks forming a thick LLBL and cold dense plasma sheet often observed during northward IMF (*Øieroset et al.*, 2005, *Li et al.*, 2009). Otherwise, reconnection takes place poleward of only one cusp, and open field lines filled with LLBL plasma can be appended to the magnetosphere (*Fuselier et al.*, 1995, 1997).

Inside the magnetosheath boundary layer, heated electrons are a good indicator of the magnetic field topology (*Fuselier et al.*, 1995, 1997, *Onsager et al.*, 2001) if reconnection occurs in the lobe sector of one or both hemispheres (*Onsager et al.*, 2001, *Lavraud et al.*, 2005, 2006). The identification of the LLBL is a difficult and complex task that requires a simultaneous evaluation of many parameters. In order to determine different regions at the magnetopause and around it, we used the magnetic field, plasma velocity, density and temperature data.

Figure 6.2 demonstrates our identification using a method of visual detection. The figure shows the observations of the THEMIS C spacecraft during an inbound passage on June 3, 2007. Based on the changes of plasma parameters and magnetic field together with ion(electron) spectra, we could define four regions: the plasma sheet, inner and outer LLBL, and magnetosheath. At the beginning of the time interval, the spacecraft is located in the magnetosheath because it observed fluctuating magnetic field less than 20 nT, moderate plasma velocity and high plasma density $\sim$ 40 cm^{-3}. The large magnetic field and very low plasma velocity from 1721 UT till the end of the selected time interval suggest that THEMIS C was in the magnetosphere (plasma sheet). Before entering the magnetosphere, the spacecraft crossed the inner and outer LLBL. The magnetosheath-like plasma together with the large magnetic field suggest that it spent the interval of 1718-1720 UT in the outer LLBL and then went to the inner LLBL where one can see the mixture of two plasma populations (magnetospheric and magnetosheath).

N–T plots

The investigation of the LLBL structure or, in other words, the LLBL spatial profile is complicated since the LLBL plasma parameters are highly variable and we are not able to distinguish spatial and temporal changes. However, *Hall et al.* (1985) reported a strong anticorrelation between the density and the temperature (i.e., mean energy) of the electrons and showed that, in this case, the temperature could be used to order magnetic field data. In an extended study, *Hall et al.* (1991) concluded that the boundary layer had inner and outer parts, similar to those first described by *Sckopke et al.* (1981). When described in terms of electron temperature, the outer part corresponded to a narrow range of relatively low temperatures but the inner part corresponded to a wide range of electron temperatures immediately above those in the outer part. Ordering based on electron temperature therefore gives a good resolution in the inner region but

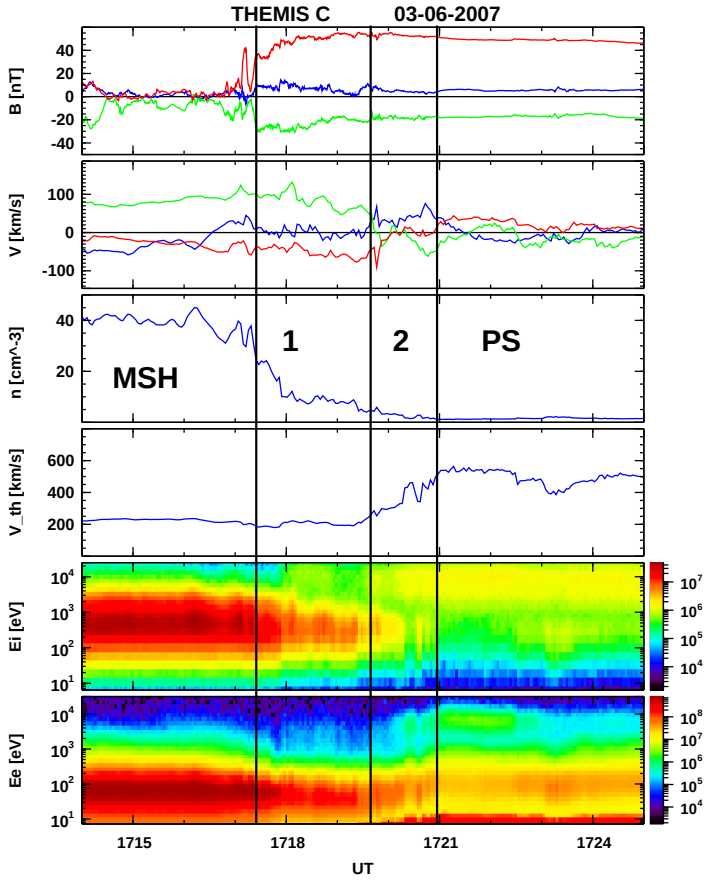

Figure 6.2: An overview of plasma parameters and magnetic field during the time interval from 1714 to 1725 UT on June 3, 2007 from THEMIS C spacecraft. From top to bottom: three components of the magnetic field, three components of the velocity vector, the ion density and thermal velocity, ions and electron spectra. Outer and inner LLBL sublayers are denoted as 1 and 2, respectively.

not in the outer region.

Based on the electron characteristics close to the Earth's dayside magnetopause, *Hapgood and Bryant* (1990), *Hall et al.* (1991), *Hapgood and Bryant* (1992a) introduced the transition parameter (TP) technique for the reordering data inside the boundary layer where the structure is complicated by the time sequence of data through multiple and partial boundary crossings caused by magnetopause motions. The transition parameter can be interpreted as a convenient measure of relative position within the boundary layer. Although not explicitly stated, this suggestion expects that the electron temperature and density are monotonous (non-linear) functions of the distance of an observer to the magnetopause. However, this assumption can be confirmed only by multi-spacecraft observations inside the LLBL.

Fear et al. (2005) studied cusp/magnetopause boundary layers structure using N–T plots and TP observed by Cluster spacecraft on the January 25, 2002. The

transition parameter was used to reorder plasma and magnetic field observations throughout this event. The procedure clarified the boundary layer structure (magnetosphere, an inner and outer boundary layer and the magnetosheath) and identified the magnetopause as the interface between the outer boundary layer and the magnetosheath. Also *Bogdanova et al.* (2008) studied the structure of the LLBL observed simultaneously near subsolar magnetopause by Double Star TC1 and mid-altitude cusp region observed by the Cluster during a prolonged interval of northward IMF. The authors observed a complicated structure of boundary layers: the plasma depletion layer, the magnetosheath boundary layer, populated by field lines newly reconnected in the lobe sector of the northern hemisphere, the LLBL, containing (1) open field lines, reconnected in the lobe sector of the northern hemisphere, (2) reclosed field lines, reconnected a second time in the lobe sector of the southern hemisphere, and (3) a transition layer, which is formed more likely by diffusion processes. They concluded that a TP technique can be successfully used for the interpretation of such a complex crossing.

Foullon et al. (2008) modified a TP technique to characterize the evolution of the magnetopause Kelvin–Helmholtz wave activity with changes of the thickness of the LLBL across the dusk flank boundary layer. The authors provided evidence of the contribution of the Kelvin–Helmholtz mechanism to the widening of the electron LLBL. Their observations were in agreement with the previous statistical study by *Mitchell et al.* (1987).

While the LLBL exhibits a density gradient normal to the magnetopause at the flanks of the magnetopause, the dayside LLBL occasionally shows a density plateau, and the LLBL may be one, two or several sublayers of an overall boundary layer (*e.g.*, *Song et al.*, 1990, 1993). For diffusive plasma entry, relatively smooth density, temperature, and flow profiles, together with close coupling to the properties of the adjacent magnetosheath are expected. On the other hand, sharp gradients bordering plateau profiles may be consequences of reconnection, although time–of–flight effects associated with reconnection may also give rise to gradual profiles of density and temperature (*Lockwood and Hapgood*, 1997). Gradual, abrupt, and plateau–like profiles of density, temperature, and flow have been found in time series of magnetopause crossings.

In the paper by ***Tkachenko*** *et al.* (2010)-A3, we focus on a spatial profile of the LLBL and the cases where this profile exhibits non–monotonous character. Our study reveals smooth and monotonous changes of the ion density and temperature over a distance of about 1 R_E under quiet upstream conditions and non-monotonous profile of the parameters during disturbed conditions that were interpreted in terms of distorted magnetopause surface.

We discussed the time interval from 1600 to 1730 on June 3, 2007. All THEMIS spacecraft moved nearly along the same orbit with a small difference between orbits that is be principal for interpretation of our results. The LLBL was observed simultaneously by four THEMIS spacecraft for a northward IMF orientation. From a solar wind monitor (Wind) observations, we can expect a stable magnetopause location until ≈1710 UT when the dynamic pressure decreases and IMF turns to a southward orientation. These two changes occurred

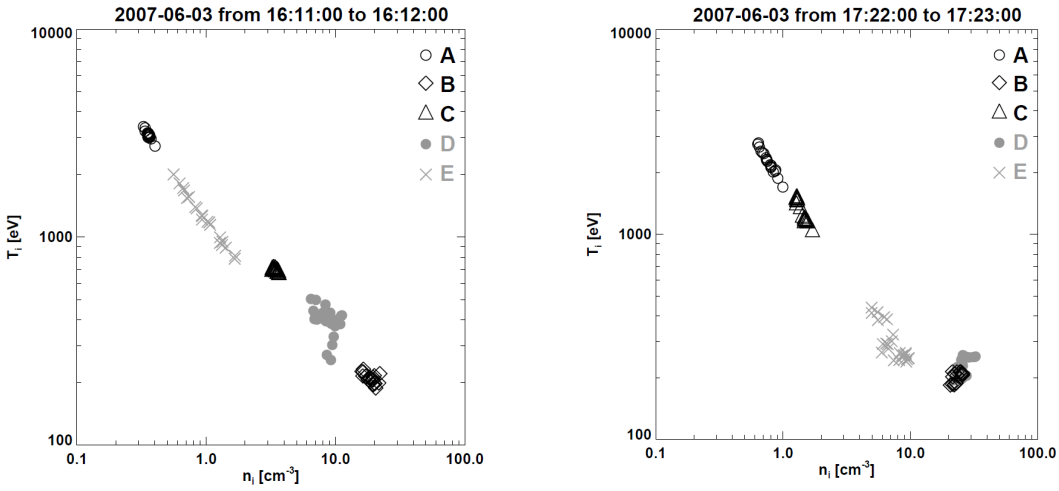

(a) (b)

Figure 6.3: Ion density vs ion temperature as measured by THEMIS under quiet (a) and disturbed (b) conditions.

nearly simultaneously but their effect would be opposite - decrease of the upstream pressure leads to the magnetopause expansion but the southward IMF erodes the dayside magnetopause and causes its inward displacement.

The changes of the IMF orientation and upstream pressure at 1710 UT led to an oscillatory motion of the magnetopause. Such motion of the magnetopause caused reformation of the LLBL profile and was confirmed by the plots of ion temperature vs ion density. In the time interval from 1611 to 1612 UT, THE, THC, and THD scanned the LLBL and the data from these three spacecraft are organized along a nearly straight line as it shown in Fig. 6.3a. The comparison with their locations with respect to the magnetopause reveals a gradually decreasing temperature and increasing density of ions from the hot and tenuous plasma-sheet population, through the boundary layer toward the cold and hot magnetosheath plasma. The changes are monotonous but the density gradient is not constant being steepest at THC and THE locations.

We have found that even under disturbed conditions, the n–T plots generally exhibit the same behavior as shown in Fig. 6.3a but one can find short intervals where the order of spacecraft apparently changes as we demonstrate in Fig. 6.3b. THA is in the plasma sheet, THB and THD are moving in the magnetosheath but THE that is farther inward from the nominal magnetopause than THC observed the colder and denser ion population. Such situation was observed only in connection with the magnetopause displacements. A projection of THEMIS orbits onto the XY_{GSM} plane with expected magnetopause deformation at 1722 UT are depicted in Fig. 6.4.

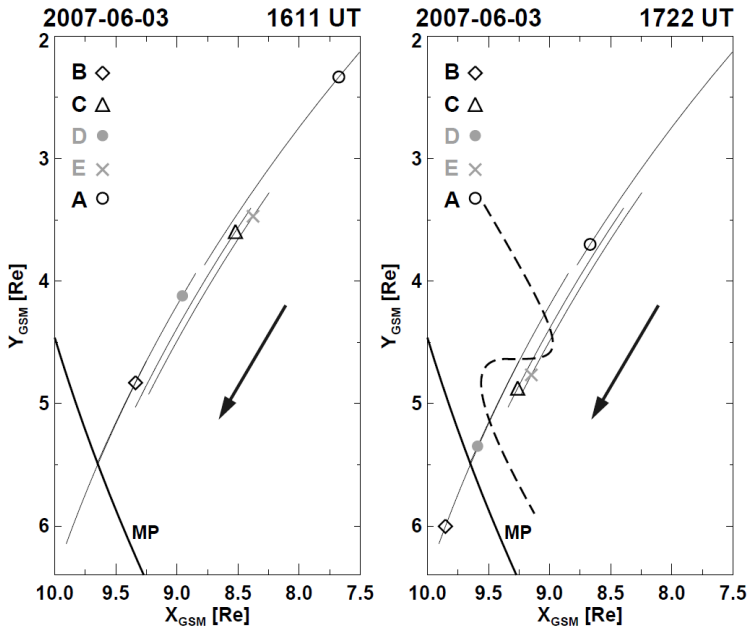

Figure 6.4: A projection of THEMIS orbits onto the XY_{GSM} plane. The points stand for locations of the spacecraft at 1611 UT (left panel) and 1722 UT (right panel); in the right panel, the full heavy line shows the model magnetopause (*Shue et al.*, 1997), and the dashed curve presents schematically the expected magnetopause deformation at 1722 UT.

Spatial profile of the LLBL

We reconstructed the radial profile of the LLBL parameters under quiet upstream conditions (***Tkachenko*** *et al.*, 2010)-A3 during a short time interval (10 min). We continue this study of the LLBL profile for the longer interval. On August 29, 2008, the THEMIS spacecraft (spacecraft coordinates in GSM at 1500 UT: THA 10.2, 1.7, -2.8; THD 10,2, -1.31, -2.8; THE 9.01, -2.2, -3.1) underwent the outbound magnetopause crossing. THC was in the solar wind (17.9, -0.5, -3.5 R_E) and was used as an upstream monitor. It registered a strong northward IMF during the selected interval (from 1230 to 1700 UT) accompanied with an increased ion density. Steady upstream conditions with northward IMF during four hours lead to the magnetopause expansion and to thickening of the LLBL (Fig. 6.5) that was ideal for investigation of the LLBL profile. We have used three–minute averages of the ion and electron density and temperature to construct the spatial profile of these parameters. The spatial coordinate is the distance from the model magnetopause that was determined from upstream observations of THC. Our reconstruction reveals that under steady upstream conditions, the LLBL conserves its spatial structure for hours.

The IMF direction plays a key role in the LLBL formation. The event analyzed in Fig. 6.6 presents a series of magnetopause crossings from THD, THE.

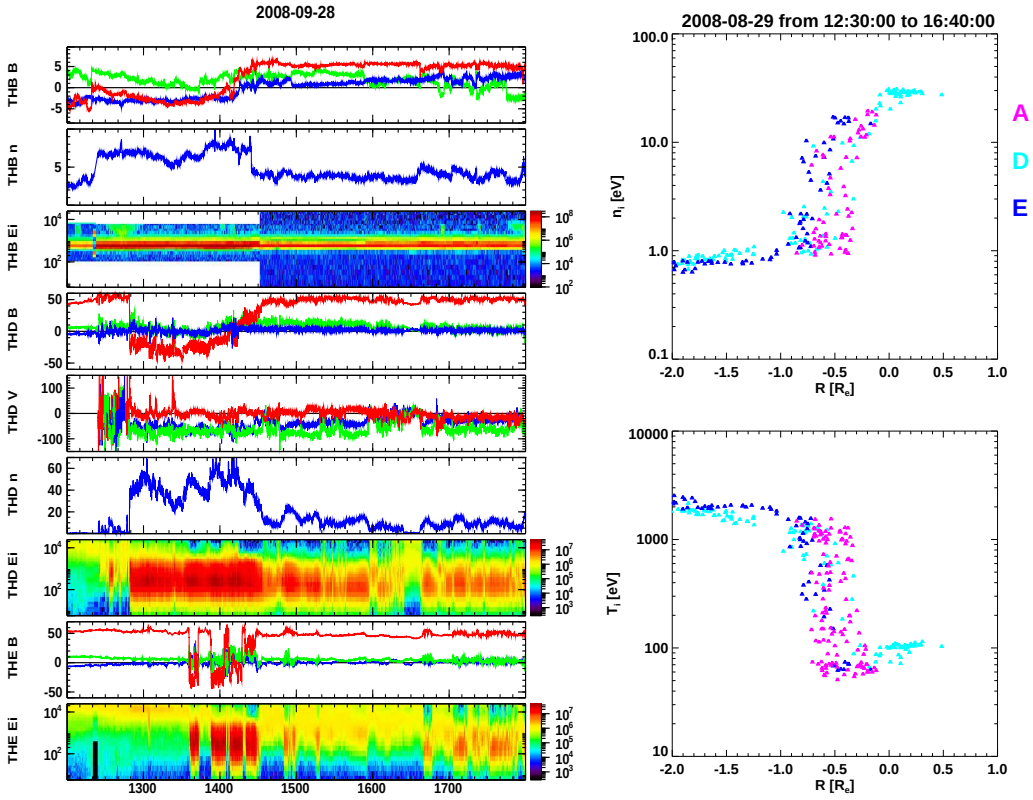

Figure 6.5: (a) Overview of the magnetic field and plasma parameters during the time interval from 1200 to 1800 UT on August 29, 2008 from THC, THD, THE, THA spacecraft. (b) Spatial profiles of the LLBL ion density and temperature.

THB a whole time was located in the solar wind and registered rotations of the IMF B_Z from southward to northward direction. N–T plots collected during intervals of southward pointing IMF consist basically of two spots: one with the cold dense magnetosheath population and the other corresponding to hot and tenuous magnetospheric population. On the other hand, there is a continuous change of plasma parameters through the layer. This change occurs in the outer part of the LLBL that is missing during intervals of southward IMF and the dayside LLBL is decoupled from the magnetosheath (Fig. 6.6b). Due to the disappearance of the outer LLBL during southward IMF, decreasing of the LLBL thickness is observed.

LLBL thickness

In order to demonstrate the effect of the southward IMF at the LLBL thickness, we analyze one LLBL crossing with change of the IMF direction in the upstream on 3 June, 2007. The summary survey of the LLBL and other regions for an analyzed event is shown in Fig. 6.7 (***Tkachenko*** *et al.*, 2008a)-A5. The color lines show the radial XY_{GSM} coordinates of five spacecraft as a function of time.

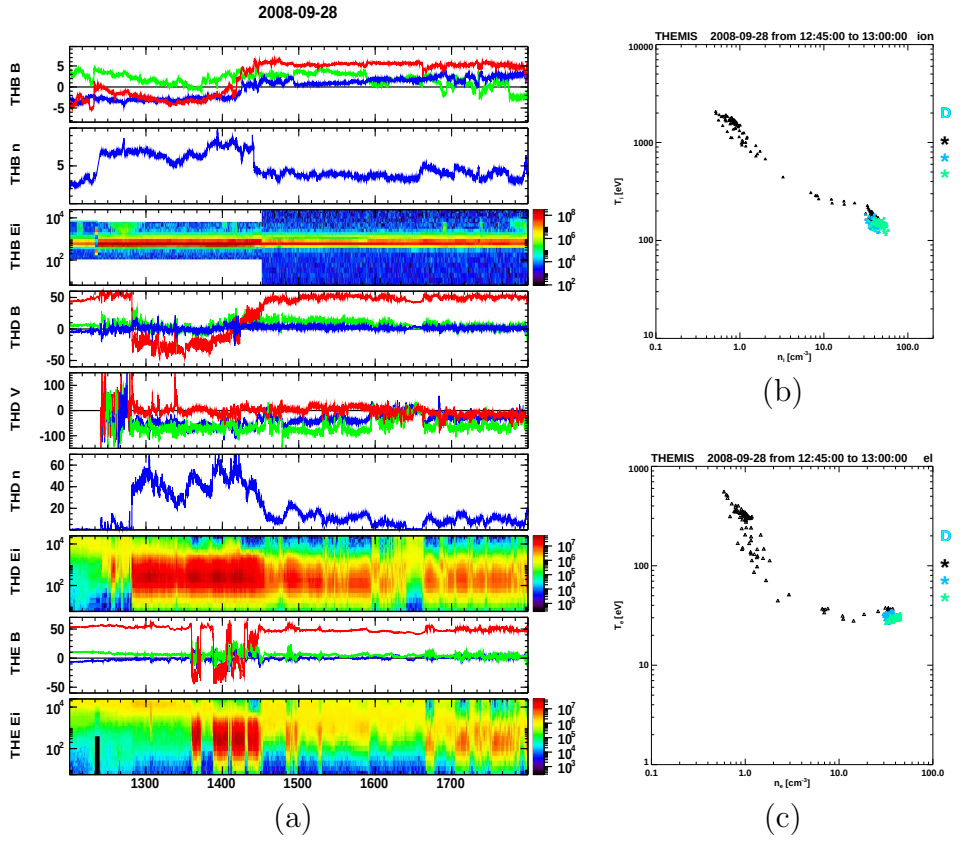

Figure 6.6: (a) Overview of the magnetic field and plasma parameters during the time interval from 1200 to 1800 UT on September 28, 2008 from THB, THD, THE spacecraft. (b,c) Ion and electron n–T plots.

Different colors distinguish various regions: the magnetosheath (green), LLBL (red), and plasma sheet (blue). The actual predicted magnetopause location computed from WIND according to the *Shue et al.* (1997) model is shown by a black line. The corresponding Wind data (solar wind dynamic pressure and IMF B_Z) are shown at the top of the figure. Source data for this drawing were the crossings of boundaries by all spacecraft, and the lines connecting consecutive crossings were roughly approximated to follow how variations of upstream conditions affect the model LLBL location. We can see that observed magnetopause crossings roughly coincide with model predictions. The figure reveals that the LLBL thickness varies in accord with the changes of the IMF orientation. If we follow the shadowed area in Fig. 6.7 we can see that THB went directly from the plasma sheet to the magnetosheath. It means that the LLBL was not present or it was very thin. The IMF as well as the magnetic field in the magnetosheath pointed southward in this time. On the other hand, at 1630 UT, IMF B_Z was positive and all spacecraft except THB observed the LLBL. This implies that the LLBL thickness was about $\sim 1.2\ R_E$. At the end of the interval, from $\sim$ 1725 UT, IMF turned to the southward orientation and the LLBL population vanished.

These observations confirm the scenario of the dayside LLBL formation by

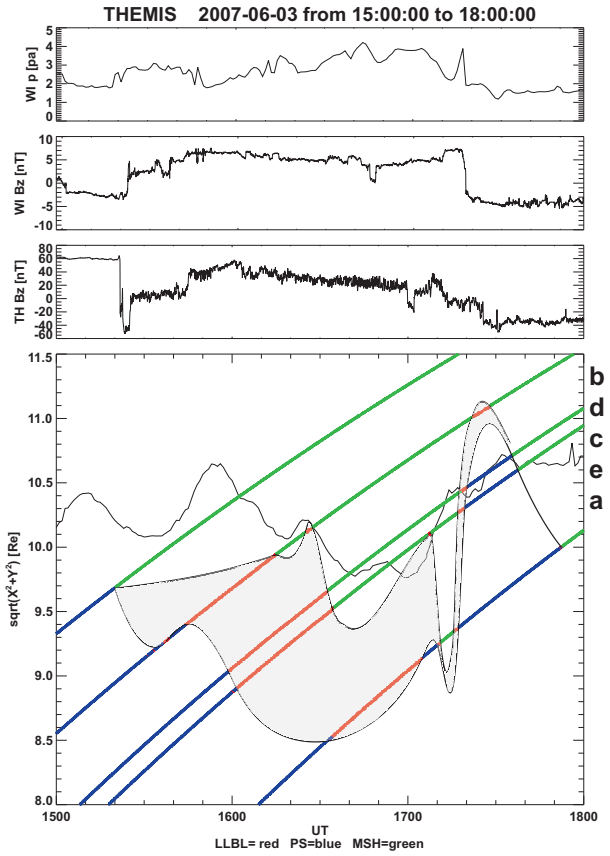

Figure 6.7: A demonstration of the LLBL thickness. From top to bottom: solar wind parameters from Wind (dynamic pressure and IMF B_Z), Z component of the magnetic field from THB, and radial XY_{GSM} coordinates as a function of time from all THEMIS spacecraft (the trajectories are marked by different colors according to the identification of visited regions).

lobe reconnection during the periods of northward IMF. The draped magnetic field lines cover the whole dayside magnetopause and reconnect tailward of one cusp. In this case, the LLBL lies on open filed lines. However, these lines can reconnect again tailward of the conjugated cusp and trap the LLBL plasma.

6.3 Transient events on the magnetopause

Fluctuations in the interplanetary magnetic field and other solar wind parameters determine the magnetopause location and its shape. A variety of transient events could also divert the magnetopause from its stationary position. Transient events are a common feature of the outer dayside magnetosphere and are connected with a number of processes including multiple rapid magnetopause crossings, a brief increase in the field component normal to the magnetopause and short enhancements of the field strength (*Sibeck*, 1995).

As we noted, some of observed transients have been referred as FTEs. Mag-

netopause motions driven by the changes of the solar–wind pressure and subsequently followed magnetopause deformation could also cause transient events. It should be noted that many of reported FTEs are examples of pressure pulse–driven magnetopause motion (*Sibeck*, 1992, 1990) because in some cases the magnetospheric signatures of FTEs and magnetic perturbations during radial magnetopause boundary motion are indistinguishable.

In ***Tkachenko*** *et al.* (2011b)–A4, we present a comprehensive analysis of one pass of the THEMIS spacecraft through the dayside low–latitude magnetopause. During the observation on August 26, 2007, THEMIS registered several quasiperiodic transients characterized by simultaneous appearance of the magnetosheath or magnetosheath-like plasma at the locations of three or four THEMIS spacecraft. None of these events exhibit FTE characteristics. Their careful analysis revealed a different nature of particular events.

An overview of observations is plotted in Fig. 6.8 where selected transients are marked as 1-5. The THEMIS fleet was leaded by THB; while THC, THD, and THE were close each other; and finally, THA followed them with a separation of about 1 R_E. The radial distances of the spacecraft from the Earth were: THB = 12.81; THC = 12.5; THD = 12.44; THE = 12.34; and THA = 11.17 R_E, respectively at 07 UT.

To analyze such observations, an actual IMF orientation is significant. However, two available upstream monitors (Wind and ACE) were located relatively far away from the Sun-Earth line so their data differ significantly and cannot be used for a reliable determination of upstream parameters. Nevertheless, despite some differences, one can note several common features in observations of all monitors. The decrease of the solar wind dynamic pressure leads to an expansion of the magnetopause that follows the outbound motion of THEMIS and thus the magnetopause remains approximately between THA and THB. Since the investigated processes would be determined by the magnetic field at a close proximity of the magnetopause, we used THB observations whenever located in the magnetosheath.

Two of selected events (events numbered 1 and 3) seem to be the magnetopause deformation caused by the sign change of IMF B_Z. During the event 1, the part of the magnetopause could be affected by a southward magnetosheath magnetic field and could be eroded by reconnection, whereas other parts do not. On the other hand, in the case of the event 3, the transient inward magnetopause motion followed after a southnorth turn of the magnetosheath B_Z was probably caused by the increase of the magnetosheath density. The deformation was highly elongated in the direction of the magnetospheric magnetic field and did not produce bipolar B_N changes when the magnetopause deformation passes the spacecraft.

Our event 2 demonstrates that the formation process of a thick boundary layer during northward pointing IMF is unsteady, especially if the B_Z component of the magnetosheath magnetic field fluctuates. The event 5 demonstrates that the formation (destruction) of a thick boundary layer is very quick when the magnetosheath magnetic field turns northward/southward. Such turns are very

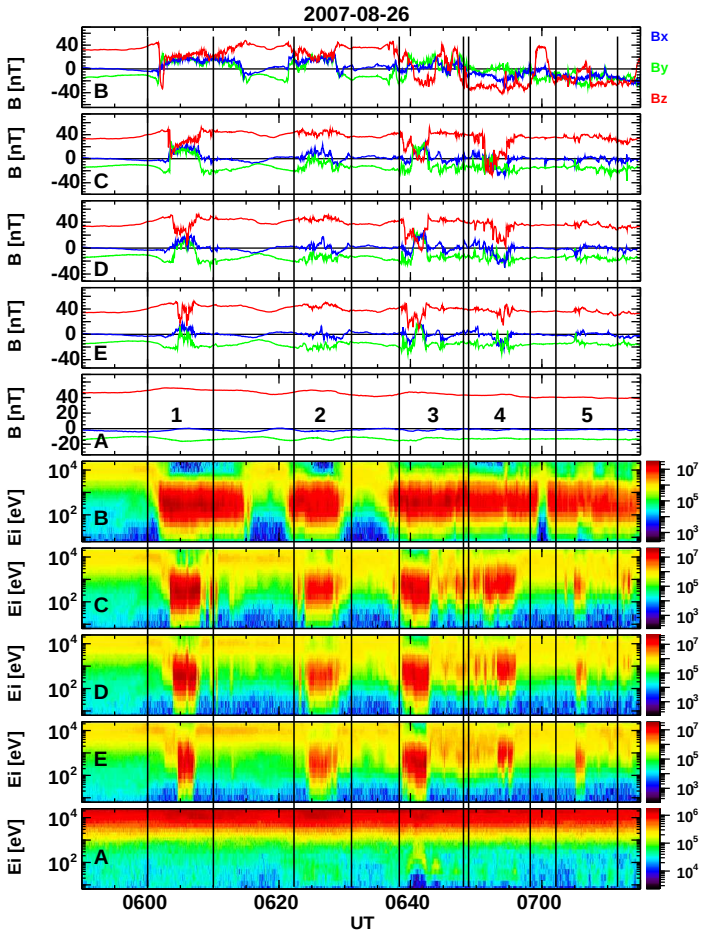

Figure 6.8: Overview of THEMIS observations on August 26, 2007 from 0550 to 0715 UT. From top to bottom: magnetic fields measured by THB; THC; THD; THE; and THA, respectively; ion spectra registered by all THEMIS probes in the same order. Our events are marked as 1-5.

frequent in the magnetosheath but observations of induced transients require an appropriate spacecraft constellation in a limited range of local times, thus they are observed sporadically.

The event 4 is identified as a crossing of the reconnection outflows. This transient shows that a negligible variation of the magnetosheath magnetic field at the magnetopause can change the location of the reconnection site or, maybe, that the reconnection site location is unstable even under steady conditions. The event occurred under a strong southward magnetosheath magnetic field that would imply steady subsolar reconnection or a periodic FTE formation (*Russell et al.*, 1996). The event does not exhibit the FTE features and the multipoint observation allowed us to estimate the thickness of the layer affected by reconnection to be $<0.6\ R_E$, *i.e.*, significantly smaller than a typical FTE cross-section (*Sonnerup et al.*, 2004). We think that a transient nature of the event is connected with a limited local time extent of the reconnection site. This site then

moves not only in the Z direction but it can shift also in the Y direction and this shift is responsible for a short-time duration of the observation. Small changes of the orientation of the magnetosheath magnetic field observed by THB are probably the proper cause of this motion.

All analyzed events were characterized by short-time enhancements of a low-energy ion population in data of three THEMIS spacecraft (THC, THD, THE). We have found three types of events but all of them were accompanied with a rotation of the magnetosheath magnetic field B_Z component. As a summary, we found three possible mechanisms of observed events: (1) magnetopause deformation, (2) LLBL thickening, and (3) pulsed reconnection.

Chapter 7

Conclusion

In this thesis, we study two key regions around the magnetopause, namely the high-altitude cusp and the LLBL. Three related topics are discussed: turbulent structures in high-latitudes as well as in the dayside magnetopause and spatial-temporal variations of the LLBL profile. Our analysis is primarily based on data from the recent space missions THEMIS and the older Interball–1 and Magion–4 project.

In the first part of the thesis, we have analyzed one interesting structure in the cusp–magnetosheath interface (***Tkachenko*** *et al.*, 2008b)-A1. Our analysis revealed that the observations are consistent with the presence of a vortex-like structure inside the magnetopause indentation with a diameter ∼1800 km. We suggest that this structure is created by the magnetosheath flow that encountered the tailward edge of the magnetopause indentation. The creation of such structures is probably a part of the process that slows down the magnetosheath flow within the cusp indentation. These structures can be observed only during stable upstream conditions because their dimensions are small and they could not be distinguished from an irregular turbulence that is typical for the high-latitude magnetopause around the cusp when the whole region is in a permanent motion.

The second part of the thesis is devoted to the study of transient events on the magnetopause. The detail analysis of a long–term pass of the THEMIS spacecraft through the dayside low–latitude magnetopause shows a series of FTE-like events, some of them with bipolar B_N signatures. For those events exhibiting clear bipolar B_N variations (***Tkachenko*** *et al.*, 2011a)-A2, we conclude that the observed features are almost consistent with two possible interpretations: destruction of the the flux rope after an IMF turn from southward to northward orientation and a local magnetopause deformation. We prefer the explanation in terms of the magnetopause deformation because it includes a rotation of B_Z in the magnetosheath and can explain enhanced flows of low energy plasma in the magnetosphere that are not accompanied with the magnetic field changes. Moreover, the magnetopause deformation can explain behavior of the magnetosheath flows.

On the other hand, for the transients with weak B_N variations (***Tkachenko***

et al., 2011b)-A4, we found different causes of the observed phenomenon. However, we have found one common source for all of them - the change of the sign of the magnetosheath B_Z component. Transients induced by a reversal of the magnetosheath magnetic field B_Z component have several peculiar features that distinguish them from the events of the same kind caused by other sources. We could conclude that: (1) A monitor of magnetosheath parameters is principal for an interpretation of magnetopause transients; (2) When B_Z is the significant magnetosheath component, the magnetopause deformation connected with a change of its sign can lead to the magnetopause deformation, similarly to that caused by an upstream pressure pulse but it does not posses the bipolar B_N signature; (3) The thickness of the boundary layer containing the magnetosheath-like plasma is controlled by the sign of the B_Z component at the magnetopause; (4) A short-time turn to the northward orientation creates a bulge of dense low-energy plasma on magnetospheric lines.

All magnetopause transients in a varying degree disturb spatial profiles of the LLBL. Using n–T plots (***Tkachenko*** *et al.*, 2010)-A3, we determine the profiles of plasma parameters under various solar wind conditions. The main attention is devoted to the influence of IMF B_Z. We have found that under quiet upstream conditions and the northward IMF orientation, the LLBL exhibits smooth and monotonous variations of the density and temperature that occur along the distance $\sim$1 R_E. Sudden changes of the upstream (magnetosheath) parameters can lead to apparently non-monotonous spatial profile of the plasma parameters, however, we believe that this effect is connected with distortion of the magnetopause surface.

N–T plots collected during intervals of southward pointing IMF consist basically of two spots: one with the cold dense magnetosheath population and the other corresponding to hot and tenuous magnetospheric population that can be attributed to an inner part of the LLBL. The outer part of the LLBL is missing during intervals of southward IMF. Due to the disappearance of the outer LLBL, decreasing of the LLBL thickness is observed (***Tkachenko*** *et al.*, 2010)-A3.

We can summarize that the thickness of the LLBL is controlled by the sign of the IMF B_Z component being narrower during intervals of southward IMF (***Tkachenko*** *et al.*, 2008a)-A5. The changes of the LLBL thickness follow almost immediately after the changes of the IMF direction. These observational facts lead to the conclusion that the main source of the LLBL plasma is reconnection proceeding in the cusp region.

References

Akasofu, S., E. W. Hones, Jr., S. J. Bame, J. R. Asbridge, and A. T. Y. Lui (1973), Magnetotail and boundary layer plasmas at geocentric distance of ~ 18 R_E: Vela 5 and 6 observations., *78*, 7257–7274, doi:10.1029/JA078i031p07257.

Alexandrova, O., A. Mangeney, M. Maksimovic, N. Cornilleau-Wehrlin, J. Bosqued, and M. André (2006), Alfvén vortex filaments observed in magnetosheath downstream of a quasi-perpendicular bow shock, *Journal of Geophysical Research*, *111*, 12,208–+, doi:10.1029/2006JA011934.

Anderson, B. J., and S. A. Fuselier (1993), Magnetic pulsations from 0.1 to 4.0 Hz and associated plasma properties in the earth's subsolar magnetosheath and plasma depletion layer, *Journal of Geophysical Research*, *98*, 1461–1479, doi:10.1029/92JA02197.

Angelopoulos, V. (2008), The THEMIS Mission, *Space Science Reviews*, *141*, 5–34, doi:10.1007/s11214-008-9336-1.

Auster, H. U., et al. (2008), The THEMIS Fluxgate Magnetometer, *Space Science Reviews*, *141*, 235–264, doi:10.1007/s11214-008-9365-9.

Bauer, T. M., R. A. Treumann, and W. Baumjohann (2001), Investigation of the outer and inner low-latitude boundary layers, *Annales Geophysicae*, *19*, 1065–1088.

Berchem, J., and C. T. Russell (1984), Flux transfer events on the magnetopause - Spatial distribution and controlling factors, *Journal of Geophysical Research*, *89*, 6689–6703, doi:10.1029/JA089iA08p06689.

Biermann, L., and A. Schlüter (1951), Cosmic Radiation and Cosmic Magnetic Fields. II. Origin of Cosmic Magnetic Fields, *Physical Review*, *82*, 863–868, doi:10.1103/PhysRev.82.863.

Boardsen, S. A., T. E. Eastman, T. Sotirelis, and J. L. Green (2000), An empirical model of the high-latitude magnetopause, *Journal of Geophysical Research*, *105*, 23,193–23,220, doi:10.1029/1998JA000143.

Bogdanova, Y. V., et al. (2005), On the formation of the high-altitude stagnant cusp: Cluster observations, *Geophysical Research Letters*, *32*, 12,101–+, doi:10.1029/2005GL022813.

Bogdanova, Y. V., et al. (2008), Formation of the low-latitude boundary layer and cusp under the northward IMF: Simultaneous observations by Cluster and Double Star, *Journal of Geophysical Research (Space Physics)*, *113*, A07S07, doi:10.1029/2007JA012762.

Bonnell, J. W., F. S. Mozer, G. T. Delory, A. J. Hull, R. E. Ergun, C. M. Cully, V. Angelopoulos, and P. R. Harvey (2008), The Electric Field Instrument (EFI) for THEMIS, *Space Science Reviews*, *141*, 303–341, doi:10.1007/s11214-008-9469-2.

Cargill, P., M. Dunlop, B. Lavraud, R. Elphic, D. Holland, K. Nykyri, A. Balogh, I. Dandouras, and H. Rème (2004), CLUSTER encounters with the high altitude cusp: boundary structure and magnetic field depletions, *Annales Geophysicae*, *22*, 1739–1754, doi:10.5194/angeo-22-1739-2004.

Chandrasekhar, S. (1981), *Hydrodynamic and hydromagnetic stability* , Dover Publications, New York.

Chapman, S., and V. C. A. Ferraro (1930), A New Theory of Magnetic Storms., *Nature*, *126*, 129–130, doi:10.1038/126129a0.

Chapman, S., and V. C. A. Ferraro (1931), a New Theory of Magnetic Storms, *Journal of Geophysical Research*, *36*, 171–186, doi:10.1029/TE036i003p00171.

Chapman, S., and H. Zirin (1957), Notes on the Solar Corona and the Terrestrial Ionosphere, *Smithsonian Contributions to Astrophysics*, *2*, 1–+.

Chen, J., and T. A. Fritz (2005), High-Altitude CUSP: The Extremely Dynamic Region in Geospace, *Surveys in Geophysics*, *26*, 71–93, doi:10.1007/s10712-005-1873-5.

Cowley, S. W. H. (1973), A qualitative study of the reconnection between the Earth's magnetic field and an interplanetary field of arbitrary orientation, *Radio Science*, *8*, 903–+, doi:10.1029/RS008i011p00903.

Crooker, N. U. (1979), Dayside merging and cusp geometry, *Journal of Geophysical Research*, *84*, 951–959, doi:10.1029/JA084iA03p00951.

Crooker, N. U., T. E. Eastman, and G. S. Stiles (1979), Observations of plasma depletion in the magnetosheath at the dayside magnetopause, *Journal of Geophysical Research*, *84*, 869–874, doi:10.1029/JA084iA03p00869.

De Keyser, J., F. Darrouzet, and M. Roth (2002), Trying to bring the magnetopause to a standstill, *Geophysical Research Letters*, *29*(10), 100,000–1, doi:10.1029/2002GL015001.

Drazin, . R. W. H., P. G. (1981), *Hydrodynamic Stability* , Cambridge University press, London.

Dungey, J. W. (1955), Electrodynamics of the outer atmosphere, *Proceedings of the ionosphere Conference*, p. 225.

Dungey, J. W. (1961), Interplanetary Magnetic Field and the Auroral Zones, *Physical Review Letters*, *6*, 47–48, doi:10.1103/PhysRevLett.6.47.

Dungey, J. W. (1963), The structure of the exosphere or adventures in velocity space, *in Geophysics The Earth's Environment, edited by C. De Witt, J. Hieblot and A. Lebeau, Eds.*, pp. 505–550.

Eastman, T. E., and E. W. Hones, Jr. (1979), Characteristics of the magnetospheric boundary layer and magnetopause layer as observed by Imp 6, *Journal of Geophysical Research*, *84*, 2019–2028.

Eastman, T. E., E. W. Hones Jr., S. J. Bame, and J. R. Asbridge (1976), The magnetospheric boundary layer - Site of plasma, momentum and energy transfer from the magnetosheath into the magnetosphere, *Geophys. Res. Let.*, *3*, 685–688.

Eastman, T. E., S. A. Fuselier, and J. T. Gosling (1996), Magnetopause crossings without a boundary layer, *Journal of Geophysical Research*, *101*, 49–58, doi: 10.1029/95JA02757.

Fairfield, D. H., A. Otto, T. Mukai, S. Kokubun, R. P. Lepping, J. T. Steinberg, A. J. Lazarus, and T. Yamamoto (2000), Geotail observations of the Kelvin-Helmholtz instability at the equatorial magnetotail boundary for parallel northward fields, *J. Geophys. Res.*, *105*, 21,159–21,174, doi: 10.1029/1999JA000316.

Farris, M. H., and C. T. Russell (1994), Determining the standoff distance of the bow shock: Mach number dependence and use of models, *Journal of Geophysical Research*, *99*, 17,681–+, doi:10.1029/94JA01020.

Fear, R. C., A. N. Fazakerley, C. J. Owen, A. D. Lahiff, E. A. Lucek, A. Balogh, L. M. Kistler, C. Mouikis, and H. Rème (2005), Cluster observations of bounday layer structure and a flux transfer event near the cusp, *Annales Geophysicae*, *23*, 2605–2620.

Ferraro, V. C. A. (1952), O the Theory of the First Phase of a Geomagnetic Storm: a New Illustrative Calculation Based on AN Idealised (plane not Cylindrical) Model Field Distribution, *Journal of Geophysical Research*, *57*, 15–49, doi:10.1029/JZ057i001p00015.

Fitzenreiter, R. J., and K. W. Ogilvie (1995), *Kelvin-Helmholtz Instability at the Magnetopause: Observations*, pp. 277–+, the American Geophysical Union.

Formisano, V. (1979), Orientation and shape of the earth's bow shock in three dimensions, *Planetary and Space Science*, *27*, 1151–1161, doi:10.1016/0032-0633(79)90135-1.

Foullon, C., C. J. Farrugia, A. N. Fazakerley, C. J. Owen, F. T. Gratton, and R. B. Torbert (2008), Evolution of Kelvin-Helmholtz activity on the dusk flank magnetopause, *Journal of Geophysical Research (Space Physics)*, *113*, A11,203, doi:10.1029/2008JA013175.

Frey, H. U., S. B. Mende, T. J. Immel, S. A. Fuselier, E. S. Claflin, J. Gérard, and B. Hubert (2002), Proton aurora in the cusp, *Journal of Geophysical Research*, *107*, 1091–+, doi:10.1029/2001JA900161.

Frey, S., V. Angelopoulos, M. Bester, J. Bonnell, T. Phan, and D. Rummel (2008), Orbit Design for the THEMIS Mission, *Space Science Reviews*, *141*, 61–89, doi:10.1007/s11214-008-9441-1.

Fujimoto, M., and T. Terasawa (1994), Anomalous ion mixing within an MHD scale Kelvin-Helmholtz vortex, *J. Geophys. Res.*, *99*, 8601–8613, doi:10.1029/93JA02722.

Fujimoto, M., and T. Terasawa (1995), Anomalous ion mixing within an MHD scale Kelvin-Helmholtz vortex. 2: Effects of inhomogeneity, *J. Geophys. Res.*, *100*, 12,025–+, doi:10.1029/94JA02219.

Fuselier, S. A., D. M. Klumpar, E. G. Shelley, B. J. Anderson, and A. J. Coates (1991), He(2+) and H(+) dynamics in the subsolar magnetosheath and plasma depletion layer, *Journal of Geophysical Research*, *96*, 21,095–+, doi:10.1029/91JA02145.

Fuselier, S. A., B. J. Anderson, and T. G. Onsager (1995), Particle signatures of magnetic topology at the magnetopause: AMPTE/CCE observations, *Journal of Geophysical Research*, *100*, 11,805–+, doi:10.1029/94JA02811.

Fuselier, S. A., B. J. Anderson, and T. G. Onsager (1997), Electron and ion signatures of field line topology at the low-shear magnetopause, *Journal of Geophysical Research*, *102*, 4847–4864, doi:10.1029/96JA03635.

Fuselier, S. A., J. Berchem, K. J. Trattner, and R. Friedel (2002), Tracing ions in the cusp and low-latitude boundary layer using multispacecraft observations and a global MHD simulation, *Journal of Geophysical Research (Space Physics)*, *107*, 1226, doi:10.1029/2001JA000130.

Fuselier, S. A., K. J. Trattner, S. M. Petrinec, C. J. Owen, and H. Rème (2005), Computing the reconnection rate at the Earth's magnetopause using two spacecraft observations, *Journal of Geophysical Research (Space Physics)*, *110*, A06,212, doi:10.1029/2004JA010805.

Gonzalez, W. D., and F. S. Mozer (1974), A quantitative model for the potential resulting from reconnection with an arbitrary interplanetary magnetic field, *Journal of Geophysical Research*, *79*, 4186–4194, doi:10.1029/JA079i028p04186.

Gosling, J. T., J. R. Asbridge, S. J. Bame, W. C. Feldman, G. Paschmann, N. Sckopke, and C. T. Russell (1982), Evidence for quasi-stationary reconnection at the dayside magnetopause, *Journal of Geophysical Research*, *87*, 2147–2158, doi:10.1029/JA087iA04p02147.

Gosling, J. T., M. F. Thomsen, S. J. Bame, T. G. Onsager, and C. T. Russell (1990), The electron edge of the low latitude boundary layer during accelerated flow events, *Geophysical Research Letters*, *17*, 1833–1836, doi:10.1029/GL017i011p01833.

Haerendel, G., G. Paschmann, N. Sckopke, and H. Rosenbauer (1978), The frontside boundary layer of the magnetosphere and the problem of reconnection, *Journal of Geophysical Research*, *83*, 3195–3216, doi:10.1029/JA083iA07p03195.

Hall, D. S., D. A. Bryant, and C. P. Chaloner (1985), Plasma variations at the dayside magnetopause, in *European Rocket & Balloon Programmes and Related Research*, *ESA Special Publication*, vol. 229, edited by T. D. Guyenne & J. Hunt, pp. 299–304.

Hall, D. S., C. P. Chaloner, D. A. Bryant, D. R. Lepine, and V. P. Tritakis (1991), Electrons in the boundary layers near the dayside magnetopause, *Journal of Geophysical Research*, *96*, 7869–7891, doi:10.1029/90JA02137.

Hapgood, M., and M. Lockwood (1995), Rapid changes in LLBL thickness, *Geophys. Res. Let.*, *22*, 77–80.

Hapgood, M. A., and D. A. Bryant (1990), Re-ordered electron data in the low-latitude boundary layer, *Geophys. Res. Let.*, *17*, 2043–2046, doi:10.1029/GL017i011p02043.

Hapgood, M. A., and D. A. Bryant (1992a), Exploring the magnetospheric boundary layer, *40*, 1431–1459, doi:10.1016/0032-0633(92)90099-A.

Hapgood, M. A., and D. A. Bryant (1992b), Exploring the magnetospheric boundary layer, *Planetary and Space Science*, *40*, 1431–1459, doi:10.1016/0032-0633(92)90099-A.

Hasegawa, H., M. Fujimoto, T. Phan, H. Rème, A. Balogh, M. W. Dunlop, C. Hashimoto, and R. TanDokoro (2004), Transport of solar wind into Earth's magnetosphere through rolled-up Kelvin-Helmholtz vortices, *Nature*, *430*, 755–758, doi:10.1038/nature02799.

Hasegawa, H., B. U. Ö. Sonnerup, C. J. Owen, B. Klecker, G. Paschmann, A. Balogh, and H. Rème (2006), The structure of flux transfer events recovered from Cluster data, *Annales Geophysicae*, *24*, 603–618, doi:10.5194/angeo-24-603-2006.

Hones, E. W., Jr., J. R. Asbridge, S. J. Bame, M. D. Montgomery, S. Singer, and S.-I. Akasofu (1972), Measurements of magnetotail plasma flow made with Vela 4B, *Journal of Geophysical Research*, *77*, 5503–5522.

Hundhausen, A. J. (1995), The solar wind, *in Introduction to Space Physics, edited by M. G. Kivelson and C. T. Russell*, pp. 91–128.

Ichimaru, S. (1973), *Basic principles of plasma physics, a statistical approach.*

Jeřáb, M., Z. Němeček, J. Šafránková, K. Jelínek, and J. Měrka (2005), Improved bow shock model with dependence on the IMF strength, *Planet. Space Sci.*, *53*, 85–93, doi:10.1016/j.pss.2004.09.032.

King, J. H., and N. E. Papitashvili (2005), Solar wind spatial scales in and comparisons of hourly Wind and ACE plasma and magnetic field data, *Journal of Geophysical Research (Space Physics)*, *110*, 2104–+, doi: 10.1029/2004JA010649.

Kivelson, M. G., and C. T. Russell (1995), Book-Received - Introduction to Space Physics, *Science*, *269*, 862–+.

Klimov, S., et al. (1997), ASPI experiment: measurements of fields and waves on board the INTERBALL-1 spacecraft, *Annales Geophysicae*, *15*, 514–527, doi:10.1007/s005850050467.

Kudela, K., V. N. Lutsenko, D. G. Sibeck, M. Slivka, T. V. Gretchko, and E. T. Sarris (2002), High energy particle dispersion events observed by interball-1 and -2, *Advances in Space Research*, *30*, 2849–2854, doi:10.1016/S0273-1177(02)80432-X.

Kuo, H., C. T. Russell, and G. Le (1995), Statistical studies of flux transfer events, *Journal of Geophysical Research*, *100*, 3513–3519, doi: 10.1029/94JA02498.

Lavraud, B., A. Fedorov, E. Budnik, A. Grigoriev, P. Cargill, M. Dunlop, H. Rème, I. Dandouras, and A. Balogh (2004a), Cluster survey of the high-altitude cusp properties: a three-year statistical study, *Annales Geophysicae*, *22*, 3009–3019, doi:10.5194/angeo-22-3009-2004.

Lavraud, B., et al. (2004b), The exterior cusp and its boundary with the magnetosheath: Cluster multi-event analysis, *Annales Geophysicae*, *22*, 3039–3054, doi:10.5194/angeo-22-3039-2004.

Lavraud, B., et al. (2005), Characteristics of the magnetosheath electron boundary layer under northward interplanetary magnetic field: Implications for high-latitude reconnection, *Journal of Geophysical Research (Space Physics)*, *110*, A06,209, doi:10.1029/2004JA010808.

Lavraud, B., et al. (2006), Evidence for newly closed magnetosheath field lines at the dayside magnetopause under northward IMF, *Journal of Geophysical Research (Space Physics)*, *111*, A05,211, doi:10.1029/2005JA011266.

Le, G., C. T. Russell, J. T. Gosling, and M. F. Thomsen (1996), ISEE observations of low-latitude boundary layer for northward interplanetary magnetic field: Implications for cusp reconnection, *Journal of Geophysical Research*, *101*, 27,239–27,250, doi:10.1029/96JA02528.

Lee, L. C., and J. V. Olson (1980), Kelvin-Helmholtz instability and the variation of geomagnetic pulsation activity, *Geophysical Research Letters*, *7*, 777–780, doi:10.1029/GL007i010p00777.

Lemaire, J., and M. Roth (1978), Penetration of solar wind plasma elements into the magnetosphere, *Journal of Atmospheric and Terrestrial Physics*, *40*, 331–335.

Lepping, R. P., et al. (1995), The Wind Magnetic Field Investigation, *Space Science Reviews*, *71*, 207–229, doi:10.1007/BF00751330.

Li, W., J. Raeder, M. Øieroset, and T. D. Phan (2009), Cold dense magnetopause boundary layer under northward IMF: Results from THEMIS and MHD simulations, *Journal of Geophysical Research (Space Physics)*, *114*, A00C15, doi:10.1029/2008JA013497.

Lin, R. P., et al. (1995), A Three-Dimensional Plasma and Energetic Particle Investigation for the Wind Spacecraft, *Space Science Reviews*, *71*, 125–153, doi:10.1007/BF00751328.

Lockwood, M., and M. A. Hapgood (1997), How the magnetopause transition parameter works, *Geophys. Res. Let.*, *24*, 373–376, doi:10.1029/97GL00120.

Lockwood, M., and J. Moen (1999), Reconfiguration and closure of lobe flux by reconnection during northward IMF: possible evidence for signatures in cusp/cleft auroral emissions, *Annales Geophysicae*, *17*, 996–1011, doi:10.1007/s005850050827.

Luhmann, J. G., R. J. Walker, C. T. Russell, N. U. Crooker, J. R. Spreiter, and S. S. Stahara (1984), Patterns of potential magnetic field merging sites on the dayside magnetopause, *Journal of Geophysical Research*, *89*, 1741–1744, doi:10.1029/0JGREA0000890000A3001741000001.

Lundin, R., et al. (2003), Evidence for impulsive solar wind plasma penetration through the dayside magnetopause, *Annales Geophysicae*, *21*, 457–472.

McComas, D. J., S. J. Bame, P. Barker, W. C. Feldman, J. L. Phillips, P. Riley, and J. W. Griffee (1998), Solar Wind Electron Proton Alpha Monitor (SWEPAM) for the Advanced Composition Explorer, *Space Science Reviews*, *86*, 563–612, doi:10.1023/A:1005040232597.

McFadden, J. P., C. W. Carlson, D. Larson, M. Ludlam, R. Abiad, B. Elliott, P. Turin, M. Marckwordt, and V. Angelopoulos (2008), The THEMIS ESA Plasma Instrument and In-flight Calibration, *Space Science Reviews*, *141*, 277–302, doi:10.1007/s11214-008-9440-2.

Mende, S. B., S. E. Harris, H. U. Frey, V. Angelopoulos, C. T. Russell, E. Donovan, B. Jackel, M. Greffen, and L. M. Peticolas (2008), The THEMIS Array of Ground-based Observatories for the Study of Auroral Substorms, *Space Science Reviews*, *141*, 357–387, doi:10.1007/s11214-008-9380-x.

Merka, J., J. Safránková, and Z. Nemecek (2002), Cusp-like plasma in high altitudes: a statistical study of the width and location of the cusp from Magion-4, *Annales Geophysicae*, *20*, 311–320, doi:10.5194/angeo-20-311-2002.

Merka, J., J. Safrankova, Z. Nemecek, and J. Simunek (2005), Magion-4 High-Altitude Cusp Study, *Surveys in Geophysics*, *26*, 57–69, doi:10.1007/s10712-005-1872-6.

Milan, S. E., M. Lester, S. W. H. Cowley, and M. Brittnacher (2000), Dayside convection and auroral morphology during an interval of northward interplanetary magnetic field, *Annales Geophysicae*, *18*, 436–444, doi:10.1007/s005850050901.

Mitchell, D. G., F. Kutchko, D. J. Williams, T. E. Eastman, and L. A. Frank (1987), An extended study of the low-latitude boundary layer on the dawn and dusk flanks of the magnetosphere, *Journal of Geophysical Research*, *92*, 7394–7404.

Miura, A. (1984), Anomalous transport by magnetohydrodynamic Kelvin-Helmholtz instabilities in the solar wind-magnetosphere interaction, *J. Geophys. Res.*, *89*, 801–818, doi:10.1029/JA089iA02p00801.

Nakamura, T. K., D. Hayashi, M. Fujimoto, and I. Shinohara (2004), Decay of MHD-Scale Kelvin-Helmholtz Vortices Mediated by Parasitic Electron Dynamics, *Physical Review Letters*, *92*(14), 145,001–+, doi:10.1103/PhysRevLett.92.145001.

Nemecek, Z., A. Fedorov, J. Safrankova, and G. Zastenker (1997), Structure of the low-latitude magnetopause: MAGION-4 observations, *Annales Geophysicae*, *15*, 553–561, doi:10.1007/s005850050471.

Newell, P. T., and C. Meng (1987), Cusp width and B(z) - Observations and a conceptual model, *Journal of Geophysical Research*, *92*, 13,673–13,678, doi:10.1029/JA092iA12p13673.

Newell, P. T., and C. Meng (1989), Dipole tilt angle effects on the latitude of the cusp and cleft/low-latitude boundary layer, *Journal of Geophysical Research*, *94*, 6949–6953, doi:10.1029/JA094iA06p06949.

Newell, P. T., and C. Meng (1994), Comment on "Unexpected features of the ion precipitation in the so-called clef/low-latitude boundary layer region: Association with sunward convection and occurrence on open field lines" by A. Nishida, T. Mukai, H. Hayakawa, A. Matsuoka, K. Tsuruda, N. Kaya, and H. Fukunishi, *Journal of Geophysical Research*, *99*, 19,609–19,614, doi: 10.1029/94JA01096.

Newell, P. T., C. Meng, D. G. Sibeck, and R. Lepping (1989), Some low-altitude cusp dependencies on the interplanetary magnetic field, *Journal of Geophysical Research*, *94*, 8921–8927, doi:10.1029/JA094iA07p08921.

Němeček, Z., and J. Safrankova (1991), The earth's bow shock and magnetopause position as a result of the solar wind-magnetosphere interaction, *Journal of Atmospheric and Terrestrial Physics*, *53*, 1049–1054.

Němeček, Z., J. Měrka, and J. Šafránková (2000), The tilt angle control of the outer cusp position, *Geophysical Research Letters*, *27*, 77–80, doi: 10.1029/1999GL010699.

Němeček, Z., J. Šimunek, J. Šafránková, and L. Prech (2004), Spatial and temporal variations of the high-altitude cusp precipitation, *Annales Geophysicae*, *22*, 2441–2450, doi:10.5194/angeo-22-2441-2004.

Němeček, Z., J. Šafránková, J. Měrka, J. Šimůnek, and L. Přech (2007), Interball contribution to the high-altitude cusp observations, *Planet. Space Sci.*, *55*, 2286–2294, doi:10.1016/j.pss.2007.05.021.

Němeček, Z., et al. (2003), Structure of the outer cusp and sources of the cusp precipitation during intervals of a horizontal IMF, *Journal of Geophysical Research (Space Physics)*, *108*, 1420–+, doi:10.1029/2003JA009916.

Nykyri, K., and A. Otto (2001), Plasma transport at the magnetospheric boundary due to reconnection in Kelvin-Helmholtz vortices, *Geophysical Research Letters*, *28*, 3565–3568, doi:10.1029/2001GL013239.

Nykyri, K., and A. Otto (2004), Influence of the Hall term on KH instability and reconnection inside KH vortices, *Annales Geophysicae*, *22*, 935–949.

Nykyri, K., P. J. Cargill, E. A. Lucek, T. S. Horbury, A. Balogh, B. Lavraud, I. Dandouras, and H. Rème (2003), Ion cyclotron waves in the high altitude cusp: CLUSTER observations at varying spacecraft separations, *Geophysical Research Letters*, *30*, 12–1, doi:10.1029/2003GL018594.

Nykyri, K., A. Otto, B. Lavraud, C. Mouikis, L. M. Kistler, A. Balogh, and H. Rème (2006), Cluster observations of reconnection due to the Kelvin-Helmholtz instability at the dawnside magnetospheric flank, *Annales Geophysicae*, *24*, 2619–2643.

Ogilvie, K. W., et al. (1995), SWE, A Comprehensive Plasma Instrument for the Wind Spacecraft, *Space Science Reviews*, *71*, 55–77, doi:10.1007/BF00751326.

Øieroset, M., J. Raeder, T. D. Phan, S. Wing, J. P. McFadden, W. Li, M. Fujimoto, H. Rème, and A. Balogh (2005), Global cooling and densification of the plasma sheet during an extended period of purely northward IMF on October 22-24, 2003, *Geophysical Research Letters*, *32*, 12–+, doi:10.1029/2004GL021523.

Onsager, T. G., J. D. Scudder, M. Lockwood, and C. T. Russell (2001), Reconnection at the high-latitude magnetopause during northward interplanetary magnetic field conditions, *Journal of Geophysical Research*, *106*, 25,467–25,488, doi:10.1029/2000JA000444.

Otto, A., and D. H. Fairfield (2000), Kelvin-Helmholtz instability at the magnetotail boundary: MHD simulation and comparison with Geotail observations, *J. Geophys. Res.*, *105*, 21,175–21,190, doi:10.1029/1999JA000312.

Owen, C. J., et al. (2001), Cluster PEACE observations of electrons during magnetospheric flux transfer events, *Annales Geophysicae*, *19*, 1509–1522, doi:10.5194/angeo-19-1509-2001.

Owen, C. J., et al. (2008), Cluster observations of "crater" flux transfer events at the dayside high-latitude magnetopause, *Journal of Geophysical Research (Space Physics)*, *113*, A07S04, doi:10.1029/2007JA012701.

Panov, E. V., J. Büchner, M. Fränz, A. Korth, S. P. Savin, H. Rème, and K. Fornaçon (2008), High-latitude Earth's magnetopause outside the cusp: Cluster observations, *Journal of Geophysical Research*, *113*, 1220–+, doi:10.1029/2006JA012123.

Parker, E. N. (1958), Dynamics of the Interplanetary Gas and Magnetic Fields., *Astrophysical Journal*, *128*, 664–+, doi:10.1086/146579.

Paschmann, G., N. Sckopke, G. Haerendel, J. Papamastorakis, S. J. Bame, J. R. Asbridge, J. T. Gosling, E. W. Hones, Jr., and E. R. Tech (1978), ISEE plasma observations near the subsolar magnetopause, *Space Sci. Rev.*, *22*, 717–737.

Paschmann, G., W. Baumjohann, N. Sckopke, I. Papamastorakis, and C. W. Carlson (1986), The magnetopause for large magnetic shear - AMPTE/IRM observations, *Journal of Geophysical Research*, *91*, 11,099–11,115, doi:10.1029/JA091iA10p11099.

Paschmann, G., W. Baumjohann, N. Sckopke, T.-D. Phan, and H. Luehr (1993), Structure of the dayside magnetopause for low magnetic shear, *Journal of Geophysical Research*, *98*, 13,409–+.

Petrinec, S. M., and C. T. Russell (1993), An empirical model of the size and shape of the near-earth magnetotail, *Geophysical Research Letters*, *20*, 2695–2698, doi:10.1029/93GL02847.

Petrinec, S. M., and C. T. Russell (1995), An examination of the effect of dipole tilt angle and cusp regions on the shape of the dayside magnetopause, *Journal of Geophysical Research*, *100*, 9559–9566, doi:10.1029/94JA03315.

Petrinec, S. M., and C. T. Russell (1996), Near-Earth magnetotail shape and size as determined from the magnetopause flaring angle, *Journal of Geophysical Research*, *101*, 137–152, doi:10.1029/95JA02834.

Phillips, J. L., et al. (1995), Ulysses Solar Wind Plasma Observations at High Southerly Latitudes, *Science*, *268*, 1030–1033, doi:10.1126/science.268.5213.1030.

Pizzo, V. J. (1985), Interplanetary shocks on the large scale - A retrospective on the last decade's theoretical efforts, *Washington DC American Geophysical Union Geophysical Monograph Series*, *35*, 51–68.

Šafránková, J., G. Zastenker, Z. Nemecek, A. Fedorov, M. Simersky, and L. Prech (1997), Small scale observation of magnetopause motion: preliminary results of the INTERBALL project, *Annales Geophysicae*, *15*, 562–569, doi:10.1007/s005850050472.

Reiff, P. H. (1984), Evidence of Magnetic Merging from Low-Altitude Spacecraft and Ground-Based Experiments, in *Magnetic Reconnection in Space and Laboratory Plasmas*, edited by E. W. Hones Jr., pp. 104–+.

Retinò, A., et al. (2006), Structure of the separatrix region close to a magnetic reconnection X-line: Cluster observations, *Geophysical Research Letters*, *33*, L06,101, doi:10.1029/2005GL024650.

Rijnbeek, R. P., S. W. H. Cowley, D. J. Southwood, and C. T. Russell (1984), A survey of dayside flux transfer events observed by ISEE 1 and 2 magnetometers, *Journal of Geophysical Research*, *89*, 786–800, doi:10.1029/JA089iA02p00786.

Roelof, E. C., and D. G. Sibeck (1993), Magnetopause shape as a bivariate function of interplanetary magnetic field B_z and solar wind dynamic pressure, *Journal of Geophysical Research*, *98*, 21,421–+, doi:10.1029/93JA02362.

Rosenbauer, H., H. Gruenwaldt, M. D. Montgomery, G. Paschmann, and N. Sckopke (1975), Heos 2 plasma observations in the distant polar magnetosphere - The plasma mantle, *Journal of Geophysical Research*, *80*, 2723–2737, doi:10.1029/JA080i019p02723.

Roux, A., O. Le Contel, C. Coillot, A. Bouabdellah, B. de La Porte, D. Alison, S. Ruocco, and M. C. Vassal (2008), The Search Coil Magnetometer for THEMIS, *Space Science Reviews*, *141*, 265–275, doi:10.1007/s11214-008-9455-8.

Russell, C. T., and R. C. Elphic (1978), Initial ISEE magnetometer results - Magnetopause observations, *22*, 681–715, doi:10.1007/BF00212619.

Russell, C. T., G. Le, and H. Kuo (1996), The occurrence rate of flux transfer events, *Advances in Space Research*, *18*, 197–205, doi:10.1016/0273-1177(95)00965-5.

Russell, C. T., G. Le, and S. M. Petrinec (2000), Cusp observations of high-and low-latitude reconnection for northward IMF: An alternative view, *Journal of Geophysical Research*, *105*, 5489–5496, doi:10.1029/1999JA900489.

Sandahl, I., et al. (1997), Cusp and boundary layer observations by interball, *Advances in Space Research*, *20*, 823–832, doi:10.1016/S0273-1177(97)00515-2.

Sauvaud, J.-A., P. Koperski, T. Beutier, H. Barthe, C. Aoustin, J. J. Thocaven, J. Rouzaud, O. Vaisberg, and N. Borodkova (1997), The INTERBALL-Tail ELECTRON experiment: initial results on the low-latitude boundary layer of the dawn magnetosphere, *Annales Geophysicae*, *15*, 587–595.

Savin, S. P., et al. (1998), Interball Tail Probe Measurements in Outer Cusp and Boundary Layers, in *Geospace Mass and Energy Flow*, edited by J. L. Horwitz, D. L. Gallagher, & W. K. Peterson, pp. 25–+.

Scholer, M., and R. A. Treumann (1997), The Low-Latitude Boundary Layer at the Flanks of the Magnetopause, *Space Science Reviews*, *80*, 341–367.

Sckopke, N., G. Paschmann, G. Haerendel, B. U. O. Sonnerup, S. J. Bame, T. G. Forbes, E. W. Hones, Jr., and C. T. Russell (1981), Structure of the low-latitude boundary layer, *Journal of Geophysical Research*, *86*, 2099–2110, doi:10.1029/JA086iA04p02099.

Shapiro, V. D., V. I. Shevchenko, P. J. Cargill, and K. Papadopoulos (1994), Modulational instability of lower hybrid waves at the magnetopause, *J. Geophys. Res.*, *99*, 23,735–+, doi:10.1029/94JA02074.

Shue, J., et al. (1998), Magnetopause location under extreme solar wind conditions, *Journal of Geophysical Research*, *103*, 17,691–17,700, doi:10.1029/98JA01103.

Shue, J.-H., J. K. Chao, H. C. Fu, C. T. Russell, P. Song, K. K. Khurana, and H. J. Singer (1997), A new functional form to study the solar wind control of the magnetopause size and shape, *Journal of Geophysical Research*, *102*, 9497–9512, doi:10.1029/97JA00196.

Sibeck, D. G. (1990), A model for the transient magnetospheric response to sudden solar wind dynamic pressure variations, *Journal of Geophysical Research*, *95*, 3755–3771, doi:10.1029/JA095iA04p03755.

Sibeck, D. G. (1992), Transient events in the outer magnetosphere - Boundary waves of flux transfer events?, *Journal of Geophysical Research*, *97*, 4009–4026, doi:10.1029/91JA03017.

Sibeck, D. G. (1995), *The Magnetospheric Response to Foreshock Pressure Pulses*, pp. 293–+, the American Geophysical Union.

Sibeck, D. G., and V. Angelopoulos (2008), THEMIS Science Objectives and Mission Phases, *Space Science Reviews*, *141*, 35–59, doi:10.1007/s11214-008-9393-5.

Sibeck, D. G., and J. T. Gosling (1996), Magnetosheath density fluctuations and magnetopause motion, *Journal of Geophysical Research*, *101*, 31–40, doi:10.1029/95JA03141.

Sibeck, D. G., L. Prech, J. Safrankova, and Z. Nemecek (2000), Two-point measurements of the magnetopause: Interball observations, *Journal of Geophysical Research*, *105*, 237–244, doi:10.1029/1999JA900390.

Smith, C. W., J. L'Heureux, N. F. Ness, M. H. Acuña, L. F. Burlaga, and J. Scheifele (1998), The ACE Magnetic Fields Experiment, *Space Science Reviews*, *86*, 613–632, doi:10.1023/A:1005092216668.

Smith, M. F., and C. J. Owen (1992), Temperature anisotropies in a magnetospheric FTE, *Geophysical Research Letters*, *19*, 1907–1910, doi:10.1029/92GL01618.

Song, P., and C. T. Russell (1992), Model of the formation of the low-latitude boundary layer for strongly northward interplanetary magnetic field, *Journal of Geophysical Research*, *97*, 1411–1420.

Song, P., C. T. Russell, R. C. Elphic, J. T. Gosling, and C. A. Cattell (1990), Structure and properties of the subsolar magnetopause for northward IMF - ISEE observations, *Journal of Geophysical Research*, *95*, 6375–6387.

Song, P., C. T. Russell, T. I. Gombosi, and D. L. DeZeeuw (2002), A model of the formation of the low-latitude boundary layer for northward IMF by reconnection: A summary and review, *Earths Low-Latitude Boundary Layer, Geophys. Monogr. Ser.*, *133*, 121–130.

Song, P., et al. (1993), Structure and properties of the subsolar magnetopause for northward interplanetary magnetic field - Multiple-instrument particle observations, *Journal of Geophysical Research*, *98*, 11,319–+, doi:10.1029/93JA00606.

Sonnerup, B. U. O. (1980), Theory of the low-latitude boundary layer, *J. Geophys. Res.*, *85*, 2017–2026, doi:10.1029/JA085iA05p02017.

Sonnerup, B. U. O., G. Paschmann, I. Papamastorakis, N. Sckopke, G. Haerendel, S. J. Bame, J. R. Asbridge, J. T. Gosling, and C. T. Russell (1981), Evidence for magnetic field reconnection at the earth's magnetopause, *Journal of Geophysical Research*, *86*, 10,049–10,067, doi:10.1029/JA086iA12p10049.

Sonnerup, B. U. Ö., H. Hasegawa, and G. Paschmann (2004), Anatomy of a flux transfer event seen by Cluster, *Geophysical Research Letters*, *31*, L11,803, doi:10.1029/2004GL020134.

Sotirelis, T., and C. Meng (1999), Magnetopause from pressure balance, *Journal of Geophysical Research*, *104*, 6889–6898, doi:10.1029/1998JA900119.

Southwood, D. J., and M. G. Kivelson (1995), Magnetosheath flow near the subsolar magnetopause: Zwan-Wolf and Southwood-Kivelson theories reconciled, *Geophysical Research Letters*, *22*, 3275–3278, doi:10.1029/95GL03131.

Southwood, D. J., M. A. Saunders, M. W. Dunlop, W. A. C. Mier-Jedrzejowicz, and R. P. Rijnbeek (1986), A survey of flux transfer events recorded by the UKS spacecraft magnetometer, *34*, 1349–1359, doi:10.1016/0032-0633(86)90071-1.

Spreiter, J. R., and B. R. Briggs (1962), On the Choice of Condition to Apply at the Boundary of the Geomagnetic Field in the Steady-State Chapman Ferraro Problem, *Journal of Geophysical Research*, *67*, 2983–2985, doi:10.1029/JZ067i007p02983.

Spreiter, J. R., A. L. Summers, and A. Y. Alksne (1966), Hydromagnetic flow around the magnetosphere, *Planetary and Space Science*, *14*, 223–+, doi:10.1016/0032-0633(66)90124-3.

Taylor, M. G. G. T., et al. (2008), The plasma sheet and boundary layers under northward IMF: A multi-point and multi-instrument perspective, *Advances in Space Research*, *41*, 1619–1629, doi:10.1016/j.asr.2007.10.013.

Tkachenko, O., J. Šafránková, and Z. Němeček (2008a), Dynamics of the LLBL thickness based on THEMIS, *WDS'08 Proceedings of Contributed Papers, Part II*, *2*, 159–167.

Tkachenko, O., J. Šafránková, Z. Němeček, J. Simunek, and L. Prech (2008b), Observations of vortex-like structure in the cusp-magnetosheath region during northward IMF orientation, *Annales Geophysicae*, *26*, 3375–3387, doi:10.5194/angeo-26-3375-2008.

Tkachenko, O., Š. Dušík, J. Šafránková, and Z. Němeček (2010), Spatial Profile of the LLBL: Multispacecraft Themis observations, *Twelfth International Solar Wind Conference*, *1216*, 487–490, doi:10.1063/1.3395909.

Tkachenko, O., J. Šafránková, Z. Němeček, and D. G. Sibeck (2011b), Dayside magnetopause transients correlated with changes of the magnetosheath magnetic field orientation, *Annales Geophysicae*, *in press.*

Tkachenko, O., J. Šafránková, Z. Němeček, and D. G. Sibeck (2011a), FTE or local magnetopause deformation?, *Geophys. Res. Let.*, *submitted.*

Treumann, R. A., J. Labelle, and T. M. Bauer (1995), *Diffusion Processes: An Observational Perspective*, 331-+ pp., the American Geophysical Union.

Trussoni, E., M. Dobrowolny, and G. Mastrantonio (1982), Kelvin-Helmholtz instability of the magnetopause boundary - Comparison with observed fluctuations, *Planetary and Space Science*, *30*, 677–685, doi:10.1016/0032-0633(82)90028-9.

Šafránková, J., J. Měrka, and Z. Němeček (2002a), Plasma flow across the cusp-magnetosheath boundary under northward IMF, *Advances in Space Research*, *30*, 2787–2792.

Šafránková, J., Z. Nemecek, S. Dusík, L. Prech, D. G. Sibeck, and N. N. Borodkova (2002b), The magnetopause shape and location: a comparison of the Interball and Geotail observations with models, *Annales Geophysicae*, *20*, 301–309, doi:10.5194/angeo-20-301-2002.

Šafránková, J., Š. Dušík, and Z. Němeček (2005), The shape and location of the high-latitude magnetopause, *Advances in Space Research*, *36*, 1934–1939, doi:10.1016/j.asr.2004.05.009.

Šafránková, J., Z. Němeček, L. Přech, J. Šimunek, D. Sibeck, and J.-A. Sauvaud (2007), Variations of the flank LLBL thickness as response to the solar wind dynamic pressure and IMF orientation, *Journal of Geophysical Research (Space Physics)*, *112*(A11), 7201–+, doi:10.1029/2006JA011889.

Šanfránková, J., Z. Němeček, D. G. Sibeck, L. Přech, J. Měrka, and O. Santolík (1998), Two point observation of high-latitude reconnection, *Geophysical Research Letters*, *25*, 4301–4304, doi:10.1029/1998GL900161.

Vaisberg, O. L., J. L. Burch, D. L. Gallagher, and N. L. Borodkova (2001), Different types of low-latitude boundary layer as observed by Interball Tail probe, *Journal of Geophysical Research*, *106*, 13,067–13,090, doi:10.1029/2000JA000154.

Vaivads, A., M. André, S. C. Buchert, J. Wahlund, A. N. Fazakerley, and N. Cornilleau-Wehrlin (2004), Cluster observations of lower hybrid turbulence within thin layers at the magnetopause, *Geophysical Research Letters*, *31*, L03,804, doi:10.1029/2003GL018142.

Velli, M. (2001), Hydrodynamics of the Solar Wind Expansion, *Astrophysics and Space Science*, *277*, 157–167, doi:10.1023/A:1012237708634.

Wang, Y., J. Raeder, and C. Russell (2004), Plasma depletion layer: Magnetosheath flow structure and forces, *Annales Geophysicae*, *22*, 1001–1017, doi:10.5194/angeo-22-1001-2004.

Zelenyi, L. M., and J. A. Sauvaud (1997), Special Topic Interball-1: first scientific results, *Annales Geophysicae*, *15*, 511–513, doi:10.1007/s005850050466.

Zhang, H., M. W. Dunlop, Q. Zong, T. A. Fritz, A. Balogh, and Y. Wang (2007), Geometry of the high-latitude magnetopause as observed by Cluster, *Journal of Geophysical Research*, *112*, 2204–+, doi:10.1029/2006JA011774.

Zhou, X., C. T. Russell, G. Le, S. A. Fuselier, and J. D. Scudder (1999), The polar cusp location and its dependence on dipole tilt, *Geophysical Research Letters*, *26*, 429–432, doi:10.1029/1998GL900312.

Zwan, B. J., and R. A. Wolf (1976), Depletion of solar wind plasma near a planetary boundary, *Journal of Geophysical Research*, *81*, 1636–1648, doi: 10.1029/JA081i010p01636.

Appendix: List of publications

A1: **Tkachenko, O.**, J. Šafránková, Z. Němeček, J. Simůnek, and L. Přech (2008), Observations of vortex-like structure in the cusp-magnetosheath region during northward IMF orientation, *Annales Geophysicae*, 26, 3375-–3387, doi:10.5194/angeo-26-3375-2008.

A2: **Tkachenko, O.**, J. Šafránková, Z. Němeček, D. G. Sibeck (2011a), FTE or local magnetopause deformation?, *Geophys. Res. Let.*, submitted.

A3: **Tkachenko, O.**, S. Dusik, J. Šafránková, and Z. Němeček (2010), Spatial Profile of the LLBL: Multispacecraft Themis observations, *American Institute of Physics Conference Series*, 1216, 487–490, doi:10.1063/1.3395909.

A4: **Tkachenko, O.**, J. Šafránková, Z. Němeček, D. G. Sibeck (2011b), Day-side magnetopause transients correlated with changes of the magnetosheath magnetic field orientation, *Annales Geophysicae*, in press.

A5: **Tkachenko, O.**, J. Šafránková, Z. Němeček (2008), Dynamics of the LLBL thickness based on THEMIS, *WDS'08 Proceedings of Contributed Papers, Part II*, 2, 159-167.

A1 – Tkachenko et al. (2008b)

Tkachenko, O., J. Šafránková, Z. Němeček, J. Simůnek, and L. Přech (2008), Observations of vortex-like structure in the cusp-magnetosheath region during northward IMF orientation, *Annales Geophysicae*, 26, 3375–3387, doi:10.5194/angeo-26-3375-2008.

A2 – Tkachenko et al. (2011a)

Tkachenko, O., J. Šafránková, Z. Němeček, and D. G. Sibeck (2011a), FTE or local magnetopause deformation?, *Geophys. Res. Let.*, submitted.

A3 – Tkachenko et al. (2010)

Tkachenko, O., S. Dusik, J. Šafránková, and Z. Němeček (2010), Spatial Profile of the LLBL: Multispacecraft Themis observations, *American Institute of Physics Conference Series*, 1216, 487–490, doi:10.1063/1.3395909.

A4 – Tkachenko et al. (2011b)

Tkachenko, O., J. Šafránková, Z. Němeček, D. G. Sibeck (2011b), Dayside magnetopause transients correlated with changes of the magnetosheath magnetic field orientation, *Annales Geophysicae*, in press.

A5 – Tkachenko et al. (2008a)

Tkachenko, O., J. Šafránková, Z. Němeček (2008), Dynamics of the LLBL thickness based on THEMIS, *WDS'08 Proceedings of Contributed Papers*, *Part II*, 2, 159-167..